

# TIP JETS AND WESTERLIES: INVESTIGATING AIR-SEA INTERACTIONS IN THE SOUTHEAST LABRADOR SEA

LEE WILLIAM COLEY

24658723

DISSERTATION SUBMITTED IN FULFILMENT OF  
THE REQUIREMENTS FOR THE DEGREE OF:

MSCi OCEANOGRAPHY

UNIVERSITY OF SOUTHAMPTON



2015

WORD COUNT: 9710

PROJECT SUPERVISOR: DR ELEANOR FRAJKA-WILLIAMS

## ABSTRACT

It is debated that mesoscale reverse tip jets caused by distortion between atmospheric flow and Greenland contribute to wintertime deep convection in the southeast Labrador Sea. Synoptic scale westerlies from the Canadian continent are argued to have greater cooling influence than reverse tip jets at this site. Quantification of air-sea interactions between reverse tip jets, westerlies and the southeast Labrador Sea will provide vital information on the ability for these wind phenomena to contribute to global ocean circulation. Using QuikSCAT satellite wind data, reverse tip jets and westerlies have been objectively identified for seven winters (October to April) from 2002-2009. Composite analysis determines the surface heat fluxes and air-sea temperature differences associated with the wind events, through use of the European Centre for Medium-Range Weather Forecasts ERA-Interim reanalysis data. Over the southeast Labrador Sea both reverse tip jets and westerlies have average wind speeds up to  $30 \text{ m s}^{-1}$ . However, reverse tip jets are determined to have low associated ocean-atmosphere heat fluxes no more than  $-150 \text{ W m}^{-2}$ , whilst westerlies drive greater cooling with heat fluxes up to  $-720 \text{ W m}^{-2}$  over single events. Associated atmospheric temperatures are the primary influence on negative heat flux magnitudes, not wind speed, with total wintertime heat fluxes correlating significantly to the mean winter air-sea temperature differences ( $r = -0.82$ ). Westerly air temperatures originating from the Canadian continent are as cold as  $-9.7 \text{ }^\circ\text{C}$ , whilst air temperatures associated with reverse tip jets originating over relatively warm oceans are no cooler than  $-1.1 \text{ }^\circ\text{C}$ . Interannual variations are seen in winter heat fluxes and temperatures, largely from the influence of the North Atlantic Oscillation (NAO). Due to low associated heat fluxes, reverse tip jets are an insignificant influence on deep convection in the southeast Labrador Sea. However, westerlies with favourable atmospheric conditions (positive NAO) drive strong ocean-atmosphere heat fluxes with potential to influence convective activity in the southeast Labrador Sea.

## ACKNOWLEDGEMENTS

A well-deserved thanks to Eleanor Frajka-Williams for her advice on data analysis and all our oceanographic discussions. Thanks also to Lena Schulze for her aid with QuikSCAT wind data trouble shooting. All data analysis was completed on Mathworks MATLAB®.

## TABLE OF CONTENTS

<b>SECTION I: INTRODUCTION</b> .....	<b>1</b>
1.1 Motivation.....	<b>1</b>
1.2 Aims.....	<b>2</b>
<b>SECTION II: BACKGROUND</b> .....	<b>4</b>
2.1 The Winds of Greenland.....	<b>4</b>
2.2 Heat Fluxes and Air-Sea Interactions.....	<b>5</b>
2.3 Current Understanding.....	<b>7</b>
<b>SECTION III: DATA</b> .....	<b>9</b>
3.1 QuikSCAT Surface Winds.....	<b>9</b>
3.1.1 Processing QuikSCAT Data.....	<b>9</b>
3.2 ERA-Interim Heat Fluxes and Air-Sea Temperatures.....	<b>10</b>
3.2.1 Processing ERA-Interim Data.....	<b>11</b>
3.3 ETOPO2v2 Bathymetry.....	<b>11</b>
3.4 Hurrell North Atlantic Oscillation.....	<b>11</b>
<b>SECTION IV: METHODS</b> .....	<b>13</b>
4.1 Identifying Tip Jets and Westerlies.....	<b>13</b>
4.2 Quantifying Air-Sea Interactions.....	<b>14</b>
4.2.1 Associated Heat Fluxes.....	<b>14</b>
4.2.2 Air-Sea Temperature Difference.....	<b>15</b>
4.3 Interannual Variability.....	<b>15</b>
<b>SECTION V: RESULTS</b> .....	<b>16</b>
5.1 Analysing Greenland’s Winds.....	<b>16</b>
5.2 Interannual Variability.....	<b>31</b>
<b>SECTION VI: DISCUSSION</b> .....	<b>40</b>
6.1 Validating Data Accuracy.....	<b>40</b>
6.2 Complexity of Tip Jets.....	<b>41</b>
6.3 Associated Heat Fluxes.....	<b>43</b>
6.4 Tip Jets and the NAO.....	<b>45</b>
6.5 Influencing Deep Convection.....	<b>46</b>
<b>SECTION VII: CONCLUSIONS</b> .....	<b>49</b>
<b>REFERENCES</b> .....	<b>51</b>

## LIST OF FIGURES AND TABLES

- FIGURE 1:** Topography of Greenland and key regions of interest, *p. 5*
- FIGURE 2:** Location of the southeast Labrador Sea, *p. 14*
- FIGURE 3:** Monthly averaged wind speeds around the location of Cape Farewell, *p. 17*
- FIGURE 4:** Monthly averaged heat fluxes around the location of Cape Farewell, *p. 18*
- FIGURE 5:** A reverse tip jet event that occurred from 0000 UTC on January 21<sup>st</sup> 2003, *p. 20*
- FIGURE 6:** A westerly event that occurred from 0000 UTC on February 17th 2003, *p. 22*
- FIGURE 7:** Wind roses of surface winds for winters 2002/2003-2008/2009 in the region of southeast Labrador Sea, *p. 23*
- FIGURE 8:** Times series of wind speed, wind direction, air-sea temperatures, and heat fluxes from the averaged region of the southeast Labrador Sea for winter 2002/2003, *p. 25*
- FIGURE 9:** Boxplots of sea surface temperature, air-temperature, wind speed, and heat flux for all reverse tip jets and westerly events in winters 2002-2009, *p. 27*
- FIGURE 10:** Scatter plot comparing total winter duration of reverse tip jets and westerlies to the total wintertime negative heat flux from the region of the southeast Labrador Sea, *p. 29*
- FIGURE 11:** Interannual variability of the winter NAO index, reverse tip jet and westerly frequency, mean winter wind speed, and mean winter air-sea temperature difference, *p. 31*
- FIGURE 12:** Scatter plot comparing winter NAO index with wintertime heat fluxes, *p. 33*
- FIGURE 13:** Scatter plot comparing mean winter wind speeds and mean air-sea temperature differences with the mean winter NAO index, *p. 33*
- FIGURE 14:** Correlation contour plot of winter mean NAO index and total winter heat flux, *p. 35*
- FIGURE 15:** Mean winter air-sea temperature difference anomalies associated with reverse tip jets, *p. 37*
- FIGURE 16:** Mean winter air-sea temperature difference anomalies associated with westerlies, *p. 39*
- TABLE 1:** Quantities of wintertime reverse tip jet and Labrador Sea air-sea interactions, *p. 28*
- TABLE 2:** Quantities of wintertime westerlies and Labrador Sea air-sea interactions, *p. 29*



*Section I***INTRODUCTION****1.1 MOTIVATION**

The subpolar gyre of the North Atlantic has exhibited large changes in temperature, salinity, and volume over recent decades, largely in response to the changing winter conditions over the Labrador Sea (Yashayaev & Loder 2008). These changes in winter conditions can be associated with global warming where model based studies predict a decline of the Atlantic meridional overturning circulation (AMOC), often due to a reduction of Labrador Sea water (LSW) formation (Stouffer et al., 2006). Investigations into the stability of the AMOC have primarily focused on the influence of freshwater on deep convection in the Labrador Sea. Coupled climate models (Jahn and Holland, 2013) have shown a weakening of the AMOC is attributable with increased freshwater input. Sources of freshwater include rapidly increasing Greenland ice melt (Mernild and Liston, 2012) and reducing Arctic sea ice (Stroeve et al., 2012), with the consequence of freshening in deep North Atlantic waters in the late 20<sup>th</sup> century (Dickson, 2002). With such evidence for a slowdown in AMOC it is important to obtain further understanding of all physical mechanisms that may control variations in the strength of wintertime deep convection in the Labrador Sea.

One physical mechanism that may influence the AMOC are the Greenland tip jets. These tip jets are intense, mesoscale, periodic atmospheric events that form off the southernmost tip of Greenland, Cape Farewell (Moore et al., 2008). Spatially these phenomena are in the meridional extent of 200 km and zonal extent of 1000 km and last for a duration of up to 48 hours (Moore & Renfrew, 2005). A global climatology of ocean surface wind speeds has revealed the waters due south of Cape Farewell as the windiest location in the world's oceans (Sampe & Xie, 2007). Wind speeds have been recorded in excess of 25 m s<sup>-1</sup>, and the driving force of such extreme atmospheric conditions are the Greenland tip jets (Martin &

Moore, 2007). It is argued that tip jets contribute to vigorous wintertime mixing and cooling of waters surrounding Cape Farewell, aiding deep convection and the consequent formation of LSW (Clark and Gascard, 1983; Moore 2003; Pickart et al. 2003) which in turn drives AMOC.

Deep convection, a process of overturning the wintertime mixed layer via strong surface cooling and mixing with colder deep waters, leads to sinking and spreading in convective plumes during winter (Lozier, 2012; Marshall and Schott, 1999). The convection of LSW is important for the exchange of heat, freshwater and biogeochemical properties between the atmosphere and abyssal ocean (Lazier et al., 2002; Yashayaev et al., 2007a; Yashayaev et al., 2007b). The meridional overturning of the North Atlantic Ocean describes the movement of water in the latitudinal/depth plane. This two-dimensional overturning involves bulk movement of upper, thermocline waters north from the equator to the pole, and the movement of deep waters in the opposing direction (Rhein et al., 2011; Talandier et al., 2014). This process, driven by the deep convection of LSW, is fundamental for the stability of global climate (Kuhlbrodt et al, 2007).

## 1.2 AIMS

This study aims to develop on the limitations of previous works through quantitatively comparing air-sea interactions between reverse tip jets, westerlies and the southeast Labrador Sea. Previous works (Sproson et al., 2008; Martin and Moore, 2007) were limited by analysis of only single events or winters. Here we will use the period of 2002-2009 comprising of seven winters. This will be achieved through using QuikSCAT wind data and the European Centre for Medium-Range Weather Forecasts ERA-Interim reanalysis (hereafter ERA-I) heat flux fields to create a time series of reverse tip jets and alternate dominant atmospheric events such as forward tip jets and westerlies (hereafter collectively referred to as westerlies). The primary finding of Sproson et al. (2008) was that robust reverse tip jets had strong ocean-atmosphere

heat fluxes associated with them, but only the westerlies had potential to contribute to deep convection. This study will consider the frequency of reverse tip jet events over entire winter periods and determine their contribution to the wintertime cooling of the Labrador Sea in comparison to westerlies. The North Atlantic Oscillation (NAO) has been determined as a major influence on interannual variations of tip jet frequency (Våge et al., 2009). Consequently, this study will evaluate the role of NAO as an influence on winter variability of ocean-atmosphere heat flux contributions by reverse tip jets and westerlies over the southeast Labrador Sea.



*Section II***BACKGROUND****2.1 THE WINDS OF GREENLAND**

Over short time scales in the winter months the high topography of Greenland (Figure 1) affects synoptic storm systems in its vicinity (Kristjánsson and McInnes, 1999; Petersen et al., 2003). The most extreme wind events are around Cape Farewell, the southern tip of Greenland. These extreme events are small scale bimodal wind phenomena with both easterly and westerly modes known as reverse tip jets and forward tip jets respectively. Other extreme wind events include barrier winds. These events arise from the impact of Greenland's imposing topography on low pressure atmospheric systems that pass this area of the northwest North Atlantic Ocean. Tip jets are narrow, stochastic high speed winds that form off Cape Farewell, while barrier winds are a geostrophic response to stable air being forced towards the high eastern coast of Greenland (Moore, 2003; Moore and Renfrew, 2005; Petersen et al., 2009). For both tip jets and barrier winds, the flow distortion arising from Greenland's high topography plays a crucial role in their formation (Våge et al., 2009a). Westerly tip jets or forward tip jets, are the result of Bernoulli acceleration down the lee slope of Greenland as well as acceleration around Cape Farewell (Doyle and Shapiro, 1999; Moore and Renfrew, 2005; Våge et al., 2009a). Alternatively, easterly tip jets or reverse tip jets appear to be the result of barrier flow undergoing an adjustment process resulting from the removal of a topographic barrier that is the eastern coast of Greenland (Moore and Renfrew, 2005; Outten et al., 2009). Barrier flows are defined by high directional consistency of the surface wind (Moore, 2003). This type of flow will occur when low Froude number flow is directed towards a topographic barrier, such as the east coast of Greenland, resulting in damming that leads to accelerated geostrophic flow parallel to the barrier (Moore and Renfrew, 2005; Harden et al., 2011).

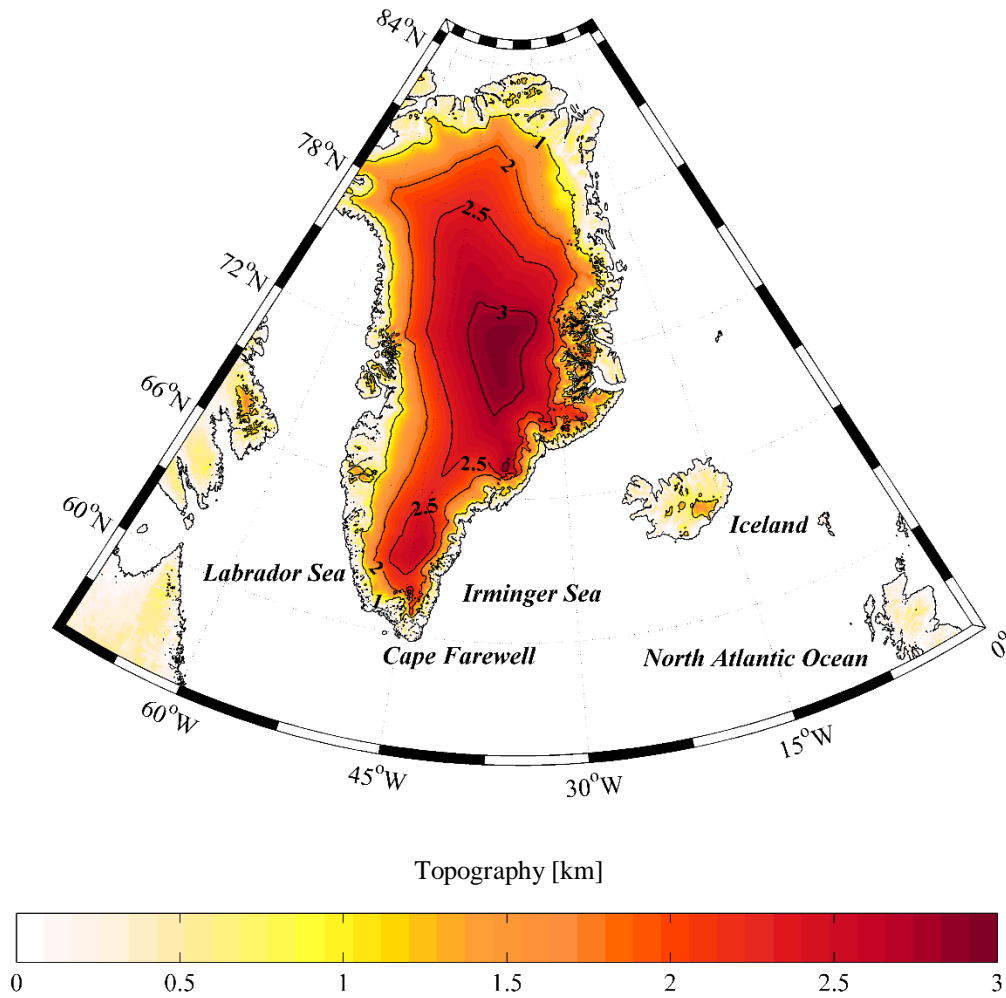


FIGURE 1: Topography of the Greenland and key regions of interest (km - shading and contours from the ETOPO2v2 bathymetry data).

## 2.2 HEAT FLUXES AND AIR-SEA INTERACTIONS

Cold dry air masses known as westerlies drive ocean-atmosphere heat fluxes that exceed  $-400 \text{ W m}^{-2}$  when prevailing over the Labrador Sea (Sproson et al., 2008). The evaporative heat loss, or latent heat loss, has a considerable impact on cooling high latitude surface waters in winter. Additionally to the latent heat loss, sensible heat is also lost from ocean-atmosphere due to large air-sea temperature differences in the event of prevailing cold dry westerlies over the Labrador Sea. It has previously been speculated that reverse tip jets may drive strong ocean-

atmosphere heat fluxes due to their high wind speeds (Moore, 2003). One method which relates turbulent heat fluxes to observable variables such as air temperature, sea surface temperature (SST) and wind speed are the bulk aerodynamic formulas:

$$\text{Sensible Heat Flux} = c_p \rho C_{DH} U_r (T_s - T_a(z_r)) \quad \text{EQUATION. 1}$$

$$\text{Latent Heat Flux} = L \rho C_{DE} U_r (q_s - q_a(z_r)) \quad \text{EQUATION. 2}$$

In these formulas  $c_p$  is the specific heat constant at pressure,  $\rho$  is the air density,  $C_{DH}$  and  $C_{DE}$  are aerodynamic transfer coefficients for temperature and humidity respectively.  $U_r$  is mean wind speed at standard height (10 m above sea level),  $T$  is temperature and  $q$  is specific humidity, with subscript  $s$  indicating values for the sea surface temperature and  $a$  for air temperature at a standard altitude,  $z_r$ , where mean variables are known (Hartmann, 1994). These formulas indicate that turbulent heat flux can be proportional to the temperature difference between the surface and air temperature, whilst also assuming the turbulent heat flux is proportional to the mean wind speed. This proposes that reverse tip jet and westerly events may drive heat fluxes with both influence from the strong wind speeds and from large air-sea temperature differences.

Extreme wind events such as reverse tip jets and westerlies share in common large vertical gradients in temperature and moisture between the cold, dry atmosphere and the comparatively warm ocean (DuVivier and Cassano, 2015). In such events large turbulent heat fluxes are possibly due to the strong temperatures gradients and gale force winds that prevail for periods of around 48 hours (Moore, 2003; Moore and Renfrew, 2005). As a result these large heat fluxes can cause water densification (Renfrew et al., 2009; Harden et al., 2011; Oltmanns et al., 2014). Current literature provides much evidence of westerlies distorting and forming forward tip jets which are suggested to force deep convection in the Irminger Sea

(Pickart et al., 2003; Våge et al., 2008; Våge et al., 2009a). However, the role of reverse tip jets driving deep convection in the southeast Labrador Sea is still debated (Lavender et al., 2002; Martin and Moore, 2007; Sproson et al., 2008; Pickart et al., 2008; Oltmanns et al., 2014).

### 2.3 CURRENT UNDERSTANDING

Tip jets were first introduced to scientific literature by Doyle and Shapiro in 1999. They commented on a narrow westerly wind which formed off Cape Farewell, consequently making the unexpected discovery of Greenland forward tip jets. Further work was completed by Moore (2003), where a climatology of tip jets was created from satellite data. Moore found that the zonal winds forming off Cape Farewell were bimodal, with observations of easterly as well as westerly winds. Consequently, the term Greenland reverse tip jet was coined to describe the easterly events (Moore, 2003). A series of studies followed the discovery of reverse tip jets, mostly with interest in the air-sea interactions between the atmospheric phenomenon and the Labrador and Irminger seas. One notable study is that by Renfrew et al. (2008), whereby tip jets were directly measured by flying a modified aircraft through the centre of associated storms. This has allowed the validity of satellite datasets to be verified. Other studies have focused on the heat fluxes associated with reverse tip jets, with aims to understand the role which tip jets contribute to the deepening of the wintertime mixed layer in the Labrador and Irminger seas (Våge, 2008).

However, there is a dispute in the scientific community as to whether reverse tip jets influence wintertime deep convection in the southeast Labrador Sea. The current understanding of the air-sea interaction between reverse tip jets and the Labrador Sea is majorly based on findings from numerical models or satellite based analysis of single events or winters. Martin and Moore (2007) found that strong heat fluxes were associated with a reverse tip jet event that coincided with a negative buoyancy flux in the Labrador Sea, whilst Sproson et al. (2008) argues that reverse tip jets do not contribute to deep convection in the Labrador Sea, but instead

cold westerly winds off the Canadian continent drive overturning. This clear divide in the scientific community highlights a lack of understanding on the role reverse tip jets play on regional and global ocean circulation.

*Section III***DATA****3.1 QUIKSCAT SURFACE WINDS**

The Quick Scatterometer, a SeaWinds instrument to replace the NSCAT instrument, was launched in June 1999 and operated until November 2009. The instrument is referred to as QuikSCAT, a scatterometer that measures near-ocean surface winds. The instrument is essentially a radar that transmits microwaves to the Earth's surface and the reflected microwaves are used to calculate surface roughness. Over oceans, surface roughness is closely correlated with near-surface wind speed and direction, hence the 10 m above sea level QuikSCAT product. The data used in this study are the level 2B twice daily gridded ocean wind vectors (Version 3 retrieval algorithm) downloaded for the period of 2002 to November 2009, available from Remote Sensing Systems at <http://www.remss.com/missions/qscat>. The data is gridded at 0.25 degrees and the wind vector fields are available twice daily according to the timing of the ascending and descending satellite swath coverage (typically available in the early morning (0600-0900 UTC) and early evening (1800-2100 UTC)).

**3.1.1 PROCESSING QUIKSCAT DATA**

The QuikSCAT level 2B wind product from Remote Sensing Systems is retrieved using the 'Ku-2001' model (Wentz et al., 2001). The data is processed for rain flagging and sea-ice detection. Wentz et al., 2001 quotes an accuracy of up to  $1 \text{ m s}^{-1}$  and  $15^\circ$  in 10 m wind speed and wind direction respectively. In comparison to buoy observations (Ebuchi et al., 2001) Renfrew et al., 2009 calculates correlation coefficients ( $r$ ) of 0.93 and 0.96-0.98 for wind speed and direction and root mean square (RMS) differences of  $1.01 \text{ m s}^{-1}$  and  $26.5$ - $18.6^\circ$ . However, on preliminary displaying of the data the rain flagging does remove regions of data that are important to the location of study. For this reason a three-step linear interpolation is used to

predict values for the unavailable areas of data. The first step is a linear interpolation in the meridional plane as a function of longitude of both U and V vectors of the level 2B data, the second step repeats this albeit making a zonal linear interpolation as a function of latitude. The final step concludes the process by taking an average of the new meridionally and zonally interpolated level 2B U and V wind vectors. With the U and V vectors processed, a final calculation is made to create a variable of wind direction. Direction is calculated through from the vector fields via trigonometry and the inverse trigonometric function arctan. This calculation is complex as when U is zero arctan cannot be used, and therefore the calculation must be adjusted dependent on the quadrant of wind direction. A simple solution to this is to calculate wind direction with the computer math library function, atan2, within the following equation:

$$\text{Wind Direction} = \left(\frac{180}{\pi}\right) \times (\text{atan2}(U, V)) \quad \text{EQUATION. 3}$$

### 3.2 ERA-INTERIM HEAT FLUXES AND AIR-SEA TEMPERATURES

ERA-I is a global atmospheric reanalysis product from the European Centre for Medium-Range Weather Forecasts' (ECMWF). The product is available from 1979 to present and uses the Integrated Forecast System, cycle 31r2 (IFS-Cy31r2). The ERA-I project was conducted partly for the preparation for a new atmospheric reanalysis to replace ERA-40. For full details of ERA-I and available fields see Berrisford et al., (2011) and Dee et al., (2012). The data fields used in this study include surface latent and sensible heat flux, 2 m above sea level temperature (hereafter air temperature), and SST. The data used in the study is downloaded from 2002 to 2009 at 0.25 degree resolution for every 12 hours at 00:00 and 12:00. The data is available from: <http://apps.ecmwf.int/datasets/data/interim-full-daily/>.

### 3.1.1 PROCESSING ERA-INTERIM DATA

The ERA-I heat flux fields are in units of  $\text{J m}^{-2}$ . For the study of heat fluxes in periods of strong wind events the data is converted to  $\text{W m}^{-2}$ . This is achieved by dividing the values of sensible and latent heat flux by the amount of seconds in the time-step interval, in this case 12 hours or 43200 seconds. The heat fluxes associated with the wind events is a combination of latent and sensible heat, thus hereafter the term heat flux will refer to the sum of the sensible and latent heat flux. Air temperature and SST data also undertook a unit conversion as the raw data is in units of Kelvin, and is converted to units of  $^{\circ}\text{C}$  by subtracting 273.16.

### 3.3 ETOPO2V2 BATHYMETRY DATA

ETOPO2v2 is a 2 minute global bathymetric data set derived primarily from satellite sea surface altimetry data and in situ data from ship based bottom depth maps. The global data set is supplied by the “Smith and Sandwell” database, available from the following website: <http://ngdc.noaa.gov/mgg/global/relief/ETOPO2/ETOPO2v2-2006/>). The U.S. National Geophysical Data Centre (NGDC) and the National Oceanic and Atmospheric Administration (NOAA) Satellite and Information Service released the dataset in 2006. This dataset is an estimation of seafloor features being projected at the sea surface and has been constructed using the US Navy’s Geosat and the European Space Agency’s ERS-1 satellite altimeters.

### 3.4 HURRELL NORTH ATLANTIC OSCILLATION INDEX

The North Atlantic Oscillation (NAO) principle component (PC) based index is used in this study. The PC component is a time series of the leading empirical orthogonal function of the sea level pressure anomalies over the  $20^{\circ}$ - $80^{\circ}\text{N}$ ,  $90^{\circ}\text{W}$ - $40^{\circ}\text{E}$  section of the North Atlantic Ocean (Hurrell, 2003). The PC component was chosen over the alternate station based index because of the better representation of NAO spatial patterns. The winter months, taken as



October-April, for 2002-2009 were extracted from the full 1982-2014 monthly data set as this study is of the winter period Greenland tip jets. The dataset was downloaded from <https://climatedataguide.ucar.edu/climate-data/hurrell-north-atlantic-oscillation-nao-index-pc-based>.

*Section IV***METHODS****4.1 IDENTIFYING TIP JETS AND WESTERLIES**

From the gridded wind data, the region of 45-50°W and 57-60°N (southeast Labrador Sea) is selected with wind data averaged across this area at each time step. With this time series of wind speed and direction, reverse tip jets are identified following Sproson et al. (2008) as periods where speeds exceeded 15 m s<sup>-1</sup> and direction was 45-135° (from the east). Westerlies are identified with the same speed threshold but with a direction of 225-315° (from the west). Reverse tip jets and westerlies are identified for winters (April-October) from 2002-2009. When the specified criteria are met within the time series of wind speed and direction, time periods in which reverse tip jets and westerlies occur can be identified. With the timings of these wind phenomena identified, composite analysis can be used to analyse the associated air-sea interactions over periods of single events and entire winters.

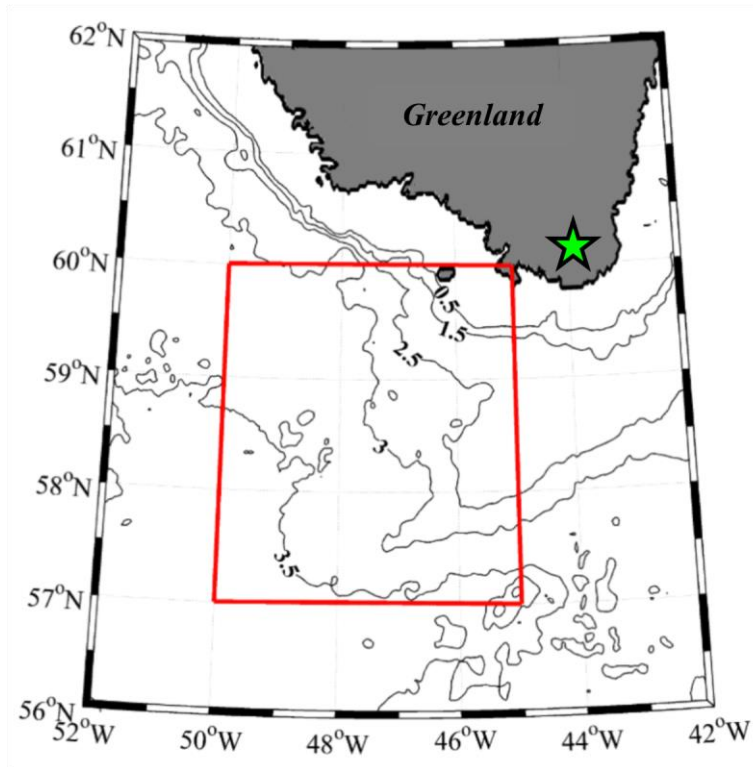


FIGURE 2: Location of southeast Labrador Sea. The region is bordered by the red box (50-45°W and 57-60°N) and Cape Farewell shown by the green star. Bathymetry is also indicated by contours (km - contours from the ETOPO2v2 bathymetry data).

## 4.2 QUANTIFYING AIR-SEA INTERACTIONS

### 4.2.1 ASSOCIATED HEAT FLUXES

The latent and sensible heat fluxes from the ERA-I data are also averaged over the southeast Labrador Sea at each time step to create time series for composite analysis. From here the sensible and latent heat flux time series can be summed to create a third time series for total heat flux (hereafter heat flux). Following this the three heat flux time series can be separated into time series for each winter period of study. Through composite analysis heat fluxes can be associated to periods of reverse tip jet and westerly events, allowing for analysis of air-sea interactions. Total wintertime heat fluxes are calculated by summing the heat flux at every time step for entire winter periods. The total wintertime contributed heat fluxes induced by the reverse tip jets and westerlies are also calculated by summing the associated heat fluxes in

periods of their occurrence. Percent contributions by reverse tip jets and westerlies to the total wintertime heat flux are also calculated.

#### 4.2.2 AIR-SEA TEMPERATURE DIFFERENCE

Data for air temperature and SST is also obtained from ERA-I. As before, the full gridded data is extracted to the area of the southeast Labrador Sea and averaged at every tip step to create time series for composite analysis. A time series of air-sea temperature difference is also created by subtracting the air temperature from the SST. Following this, the data are then separated into time series for the seven winter periods. Composite analysis is then used to identify the air temperature and SST associated with the reverse tip jet and westerly events.

### 4.3 INTERANNUAL VARIABILITY

The winter months of October to April have been extracted from the Hurrell monthly NAO index to provide seven winters of data from 2002/2003-2008/2009. Values for average winter NAO index were also calculated by taking the mean of winter months (October-April) for consecutive years (e.g. 2002 and 2003). The NAO index data was then used for statistical analysis of interannual variability between the NAO and atmospheric phenomenon such as the reverse tip jets and westerlies. Linear relationships between the NAO and quantities such as total wintertime heat flux, winter mean wind speed and air-sea temperature difference are tested through calculation of correlation coefficients ( $r$ ). The statistical significance of  $r$  values are then quantified through a two-tailed calculation of Pearson's significance ( $p$ ), where values of less than 0.05 determine the relationship being tested as 95% significant.

*Section V***RESULTS****5.1 ANALYSING GREENLAND'S WINDS**

The monthly means of seven years of QuikSCAT data from 2002-2009 (Figure 3) reveal the spatial and temporal distribution of strong mesoscale wind phenomena. The strongest winds occur in October-April. Spatially, the strongest winds form off the south of Cape Farewell, a site of tip jet formation. The monthly mean heat fluxes are also displayed (Figure 4) whereby the strongest heat fluxes are also seen through October-April. Spatially, the heat fluxes are enhanced in a zonal band south of Cape Farewell, extending both to the east and west. This pattern corresponds well to the pattern of strong wind speeds that are also seen extending zonally from Cape Farewell. The month of January (Figure 3 and 4(a)) displays the strongest monthly mean wind speeds of up to  $15 \text{ m s}^{-1}$ , coinciding with the strongest mean heat fluxes of  $-200 \text{ W m}^{-2}$ . The months of November, December, February, and March (Figure 4 and 5(b, c, k, and l)) also show strong consistency between the spatial location of high wind speeds and the strongest heat fluxes. The maximum heat fluxes occur in the southeast Labrador Sea ( $-150$  to  $-180 \text{ W m}^{-2}$ ), with less zonal extension to the east of Cape Farewell (Figure 4(b, c and l)). These patterns indicate tip jet activity is dominant in the winter months, and the zonal band of high heat fluxes extending both east and west of Cape Farewell imply an important influence from both reverse tip jets and westerlies. Through April to September, wind speeds are weaker but the location of Cape Farewell still remains a centre of action for the stronger winds ( $8-10 \text{ m s}^{-2}$ ). The summer months coincide with the lowest ocean-atmosphere heat fluxes, with little evidence of enhancement in the area of tip jets (Figure 3 and 4(d to i)).

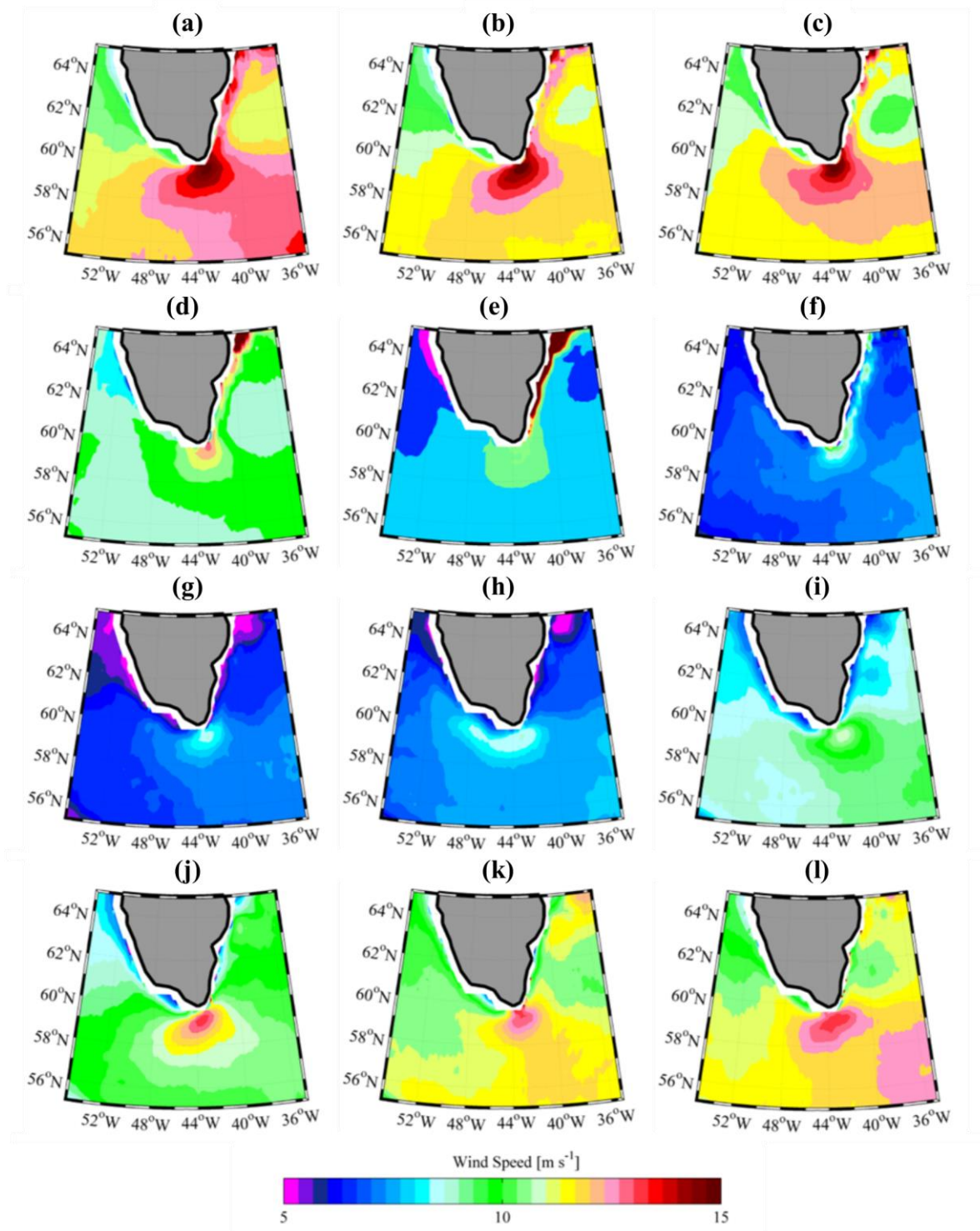


FIGURE 3: Monthly averages of QuikSCAT derived wind speed ( $\text{m s}^{-1}$ ) around the location of Cape Farewell. Plots a-l are the months January to December. Averages taken as the mean wind speed for all months within the period of 2002 to 2009.

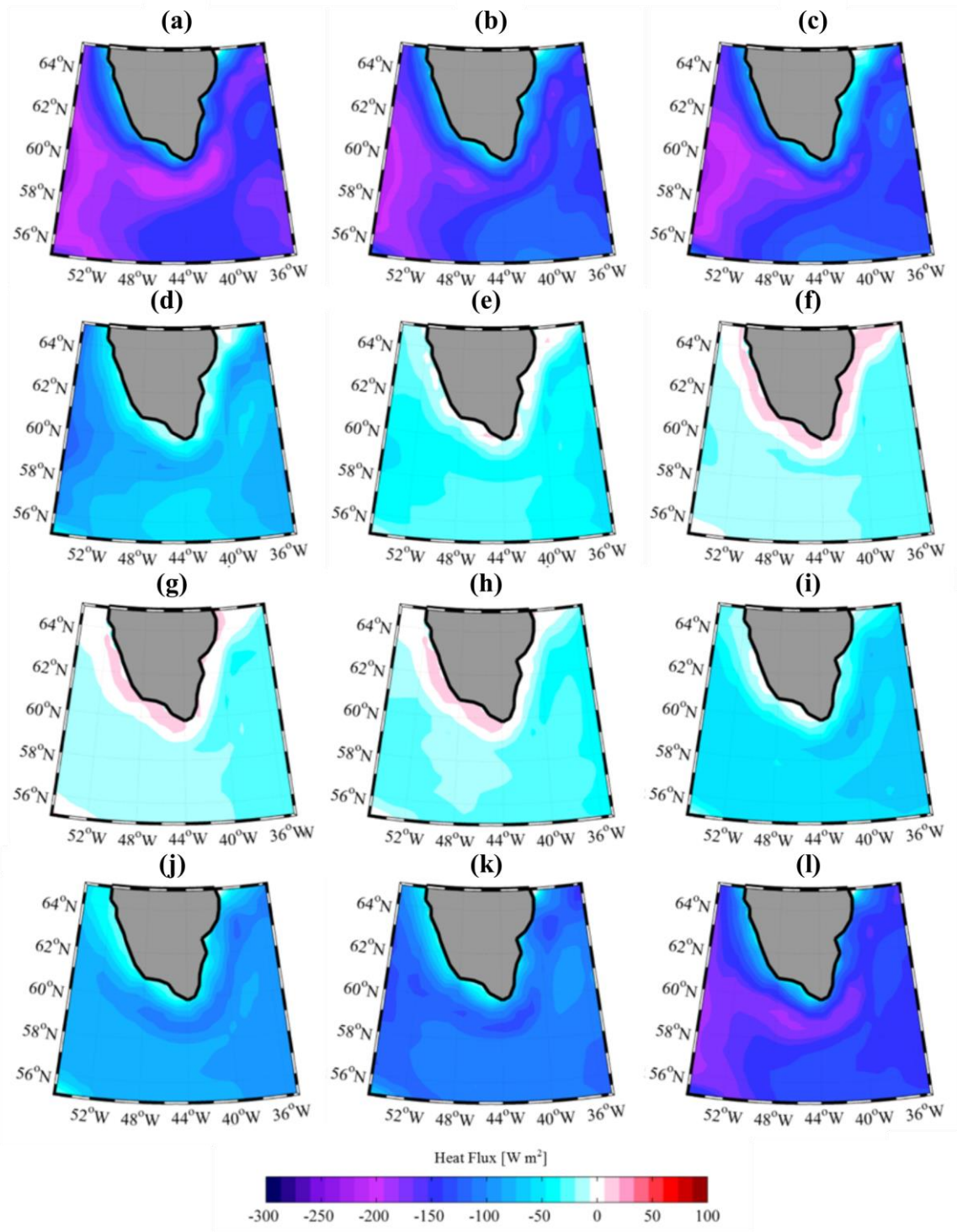


FIGURE 4: Monthly averages of ERA-I derived heat fluxes ( $\text{W m}^{-2}$ ) around the location of Cape Farewell. Plots a-l are the months January to December. Averages taken as the mean heat flux for all months within the period of 2002 to 2009.

An example of a reverse tip jet event is that which occurred on the 21<sup>st</sup> January 2003, where the formation and the progression of the tip jet from 0000 UTC on the 21<sup>st</sup> for 36 hours in 12 hour intervals is shown (Figure 5(a-c)). Initially, a strong easterly wind is dominant over the central Labrador Sea (Figure 5(a)). 12 hours later strong winds with speeds of 15-20 m s<sup>-1</sup> have formed along the southeast coast of Greenland which accelerates and spins off cyclonically with the passing of Cape Farewell (Figure 5(b)). The result of this is a reverse tip jet with maximum wind speeds of over 30 m s<sup>-1</sup> that continue to persist and strengthen within another 12 hours (Figure 5(c)) before dissipating by January 23<sup>rd</sup>. The associated heat fluxes (Figure 5(d-f)) can be seen to strengthen with the development of the reverse tip jet (Figure 5(a-c)). The heat flux is negative in the region of the southeast Labrador Sea and strengthens over the 36 hour period, reaching a maximum negative heat flux from ocean to atmosphere of -450 W m<sup>-2</sup> at its epicentre (Figure 5(f)). Additionally to the strong heat flux in the southeast Labrador Sea strong negative heat fluxes and wind speeds are also seen along the eastern coast of Greenland, suggesting the presence of barrier flow feeding the reverse tip jet (Figure 5(b and e)).



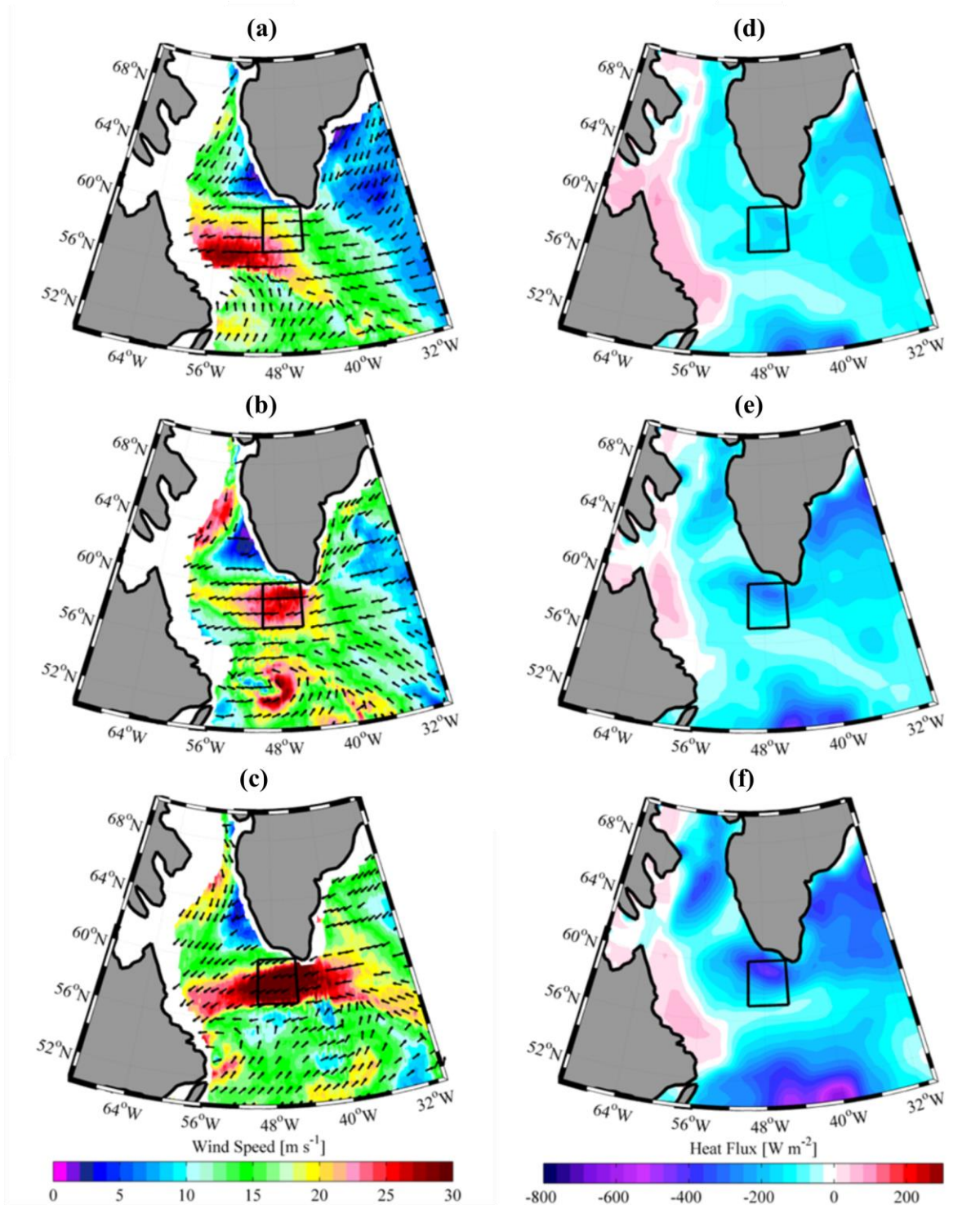


FIGURE 5: A reverse tip jet event that occurred from 0000 UTC on January 21<sup>st</sup> 2003. Plots a-c show QuikSCAT derived wind speed ( $\text{m s}^{-1}$ ) and direction (represented by arrows) at 12 hourly intervals, whilst d-f are the associated ERA-I derived heat fluxes ( $\text{W m}^{-2}$ ) for a-c respectively. The black box bounds the area of southeast Labrador Sea.

A westerly event is tracked for 36 hours at 12 hour intervals (Figure 6(a-c)) from 0000 UTC on the 17<sup>th</sup> February 2003. A strong westerly wind regime across the entire Labrador Basin with average speeds of around  $15 \text{ m s}^{-1}$  is shown (Figure 6(a)). At this point a forward tip jet is seen in its juvenile stage, but showing signs of being an extremely strong event with maximum wind speeds reaching  $30 \text{ m s}^{-1}$  to the south of Cape Farewell. 12 hours later (Figure 6(b)) an archetypal forward tip jet is shown occurring over the Irminger Sea with wind speeds exceeding  $40 \text{ m s}^{-1}$ . Another 12 hours on (Figure 6(c)) the event begins to weaken, but has spun anticyclonically to the northeast. Throughout the event strong westerly winds have persisted over the Labrador and Irminger seas, and the associated heat fluxes are accordingly strong. The negative heat fluxes associated with the westerly event are shown in Figure 6(d-f), where cooling occurs with negative heat fluxes of around  $-500 \text{ W m}^{-2}$  across the entire Labrador Sea. A maxima of  $-800 \text{ W m}^{-2}$  is seen over the Irminger Sea persisting for 24 hours (Figure 6(e-f)). Figures 5 and 6 highlight differences in associated heat fluxes between reverse tip jet and westerly events. Although the wind speeds of both events are strong (exceeding  $30 \text{ m s}^{-1}$  in both cases), the associated heat fluxes are dissimilar. The ocean-atmosphere cooling in the westerly event (Figure 6) is spatially more extensive with strong fluxes across the entire Labrador Basin. However, the cooling in the reverse tip jet event (Figure 5) is restricted to the southeast Labrador Sea with maximum heat fluxes  $350 \text{ W m}^{-2}$  lower than the westerly maximum heat flux.

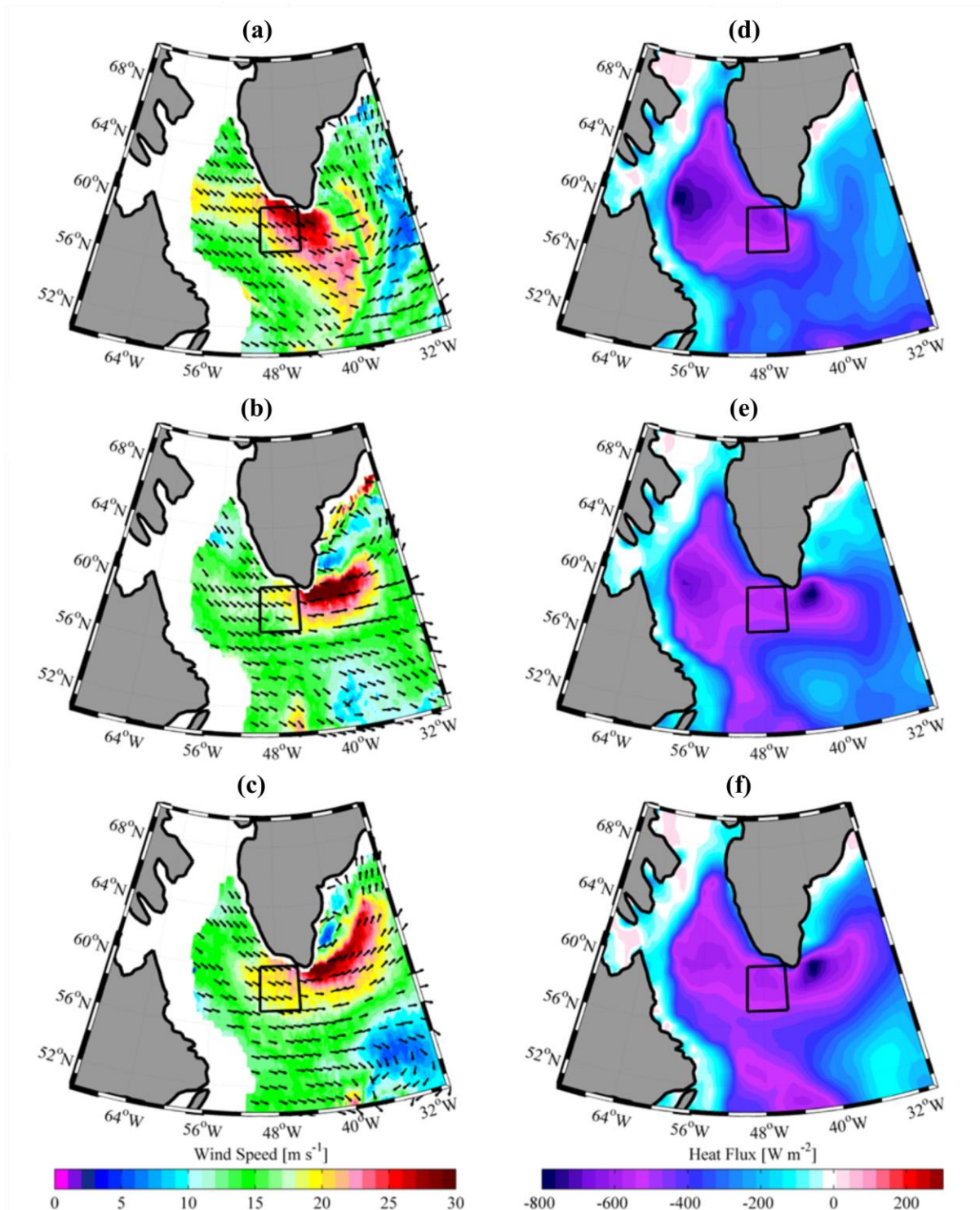


FIGURE 6: A westerly event that formed into forward tip jet occurring from 0000 UTC on February 17<sup>th</sup> 2003. Plots a-c show QuikSCAT derived wind speed ( $\text{m s}^{-1}$ ) and direction (represented by arrows) at 12 hourly intervals, whilst d-f are the associated ERA-I derived heat fluxes ( $\text{W m}^{-2}$ ) for a-c respectively. The black box bounds the area of the southeast Labrador Sea.

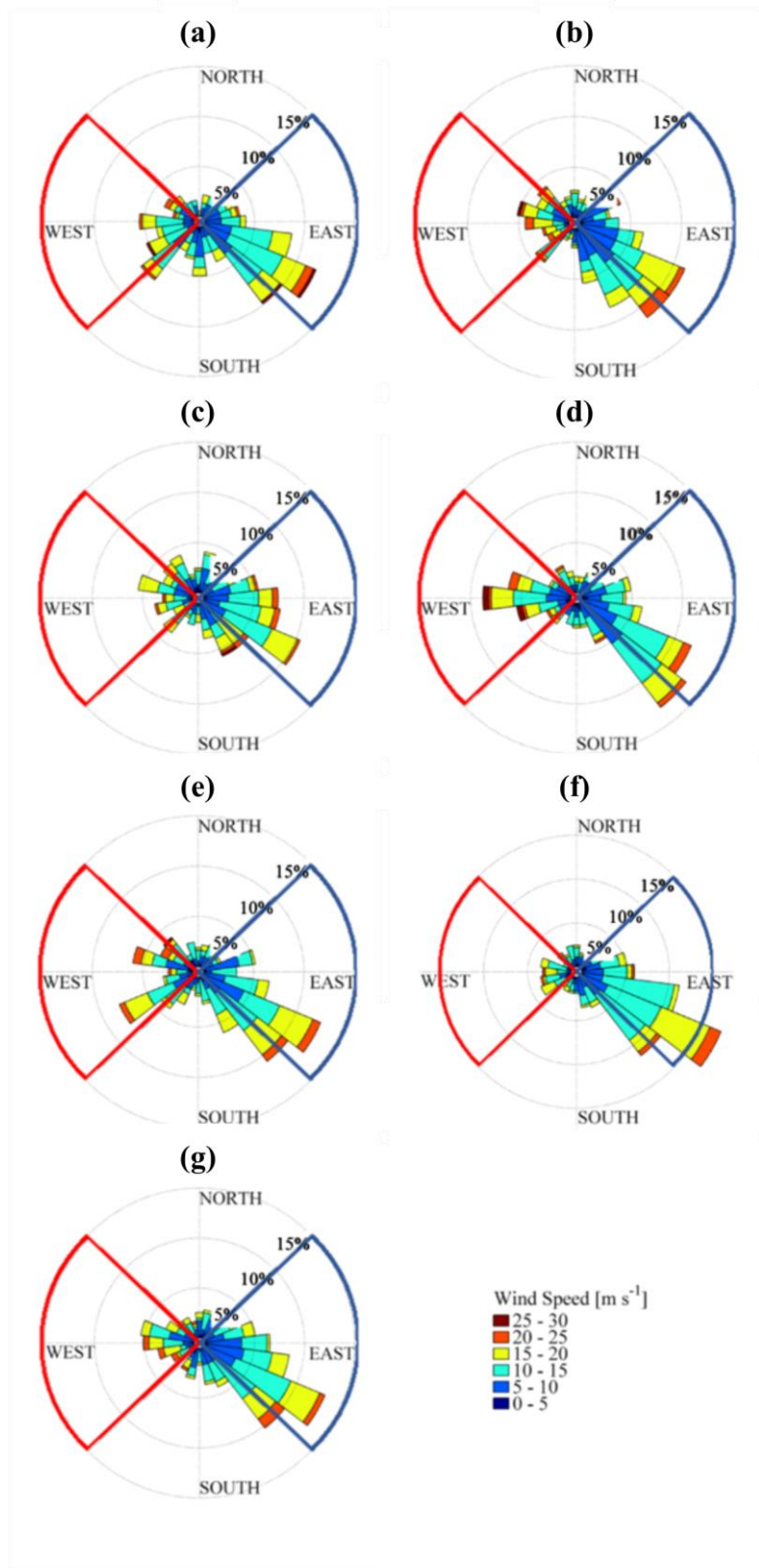
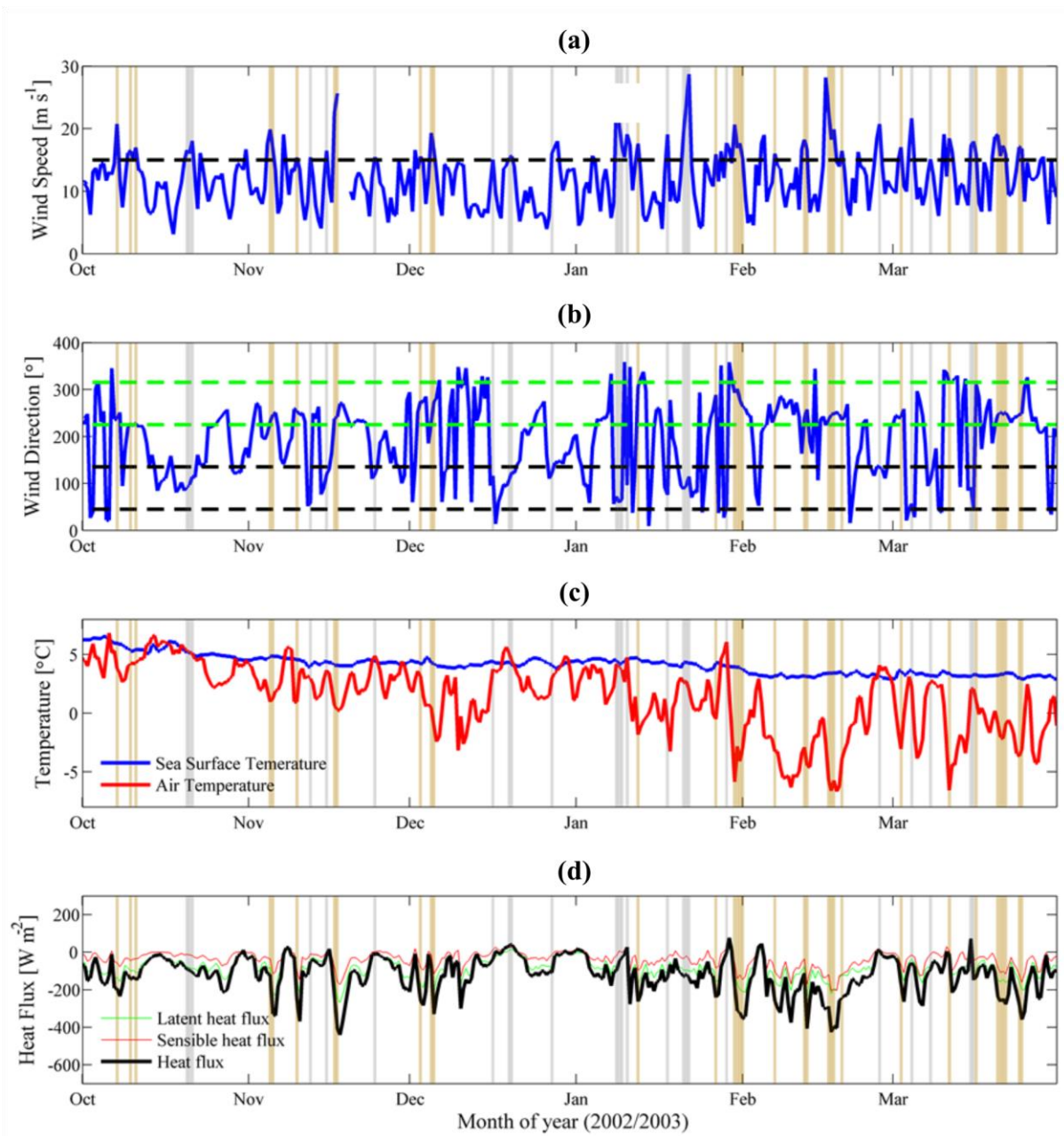


FIGURE 7: Wind roses of QuikSCAT derived surface winds ( $\text{m s}^{-1}$ ) for winters 2002/2003 to 2008/2009 (a-g respectively) in the region of southeast Labrador Sea ( $45\text{-}50^{\circ}\text{W}$  and  $57\text{-}60^{\circ}\text{N}$ ). The red segment highlights reverse tip jet identification (from  $45\text{-}135^{\circ}$  east), and the blue segment is the equivalent for westerly identification (from  $225\text{-}315^{\circ}$  west).

To characterise the different wind regimes, wind roses identify the frequency of events in regards to their speed and direction (Figure 7) from the averaged location of the southeast Labrador Sea. The most dominant wind pattern shown in all wind roses (Figure 7 (a-g)) is a high frequency of winds bearing to the west and southwest, being the main direction of over 30% of winds in the winter period of October-April. The second dominant direction of winds is those from the east, yet these patterns are more variable in frequency than the winds originating from the west. There are fewer events of northerly and southerly direction, perhaps due to the large topographic barrier of Greenland. These results show a frequent reoccurrence of winds in both the easterly and westerly directions, and both wind regimes show events with magnitudes above the  $15 \text{ m s}^{-1}$  thresholds to qualify as reverse tip jets or westerlies. These winds are represented by the yellow, orange and red colours of the wind roses and identify multiple reoccurrences of reverse tip jet and westerly events through the winters of 2002-2009.



**FIGURE 8:** Time series of wind speed, wind direction, air-sea temperatures, and heat fluxes from the averaged region of the southeast Labrador Sea for the winter of 2002/2003. Plot a shows wind speed ( $\text{m s}^{-1}$ ) with the black dashed line representing the  $15 \text{ m s}^{-1}$  threshold for reverse tip jets and westerlies. Plot b shows wind direction with black dashed lines showing the limits for reverse tip jets ( $45\text{-}135^{\circ}$  east) and the green dashed lines showing limits for westerlies ( $225\text{-}315^{\circ}$  west). Plot c shows SST ( $^{\circ}\text{C}$ ) in blue and air temperature ( $^{\circ}\text{C}$ ) in red. Plot d shows latent heat flux ( $\text{W m}^{-2}$ ) in green, sensible heat flux ( $\text{W m}^{-2}$ ) in red, and the sum of both ( $\text{W m}^{-2}$ ) in black. The vertical silver and gold bars identify reverse tip jets and westerlies respectively.

By construction, reverse tip jets and westerlies differ in wind direction (Figure 8(b)), however time series further identify differences in associated air-sea temperature differences (Figure 8(c)) and heat fluxes (Figure 8(d)). In particular, during westerlies, air temperatures are much colder than during reverse tip jets. An overall trend of increasing air temperature-SST differences is seen over the entire winter period (Figure 8(c)). However, over daily timescales there are variations in air-sea difference between reverse tip jet and westerly events. On the occasions of reverse tip jets there is negligible difference between the air temperature and the SST, whilst in westerly events air temperature is increasingly cooler than SST through the duration of winter. In late October air temperatures are cooler than SST by approximately 2-3 °C during westerlies. By late winter around February, westerly air temperatures are as much as 9 °C colder than SST. On the contrary, reverse tip jets prove to experience similar air temperatures to SST, and on some occasions air temperature is actually greater. This has an important impact on the surface heat flux that occurs when either a reverse tip jet or a westerly prevails over the southeast Labrador Sea. The analysis indicates the strongest negative heat fluxes occur in periods of westerlies (Figure 8(d)), when air temperatures are considerably lower than SST. On these occasions westerlies cause negative heat fluxes in the southeast Labrador Sea of up to  $-420 \text{ W m}^{-2}$ , whilst the reverse tip jet events with warmer air temperatures drive maximum heat fluxes of no greater than  $-150 \text{ W m}^{-2}$ .

Boxplots show the median value for SST, air temperature, wind speed, and heat flux of all reverse tip jet and westerly events of winters 2002-2009. SST is consistent between both wind phenomena, with a median of  $3.7^\circ\text{C}$  (Figure 9(a)). Air temperature however is shown to be far cooler for westerlies compared to reverse tip jets with median temperatures of  $-1.7^\circ\text{C}$  and  $3.8^\circ\text{C}$  respectively (Figure 9 (b)). Only a minority of reverse tip jets have negative associated air temperatures with the coldest at  $-1.1^\circ\text{C}$ , whilst westerlies have primarily negative associated temperatures with a minimum of  $-9.7^\circ\text{C}$ . Wind speeds (Figure 9(c)) for

both wind phenomena have median wind speeds between 17.8 and 18  $\text{m s}^{-1}$ . The median heat fluxes for reverse tip jets and westerlies are  $-56.9$  and  $-311.5 \text{ W m}^{-2}$  respectively (Figure 9(d)). Westerlies are shown to drive far greater ocean-atmosphere heat fluxes than reverse tip jets with maximum heat fluxes of up to  $-718.7 \text{ W m}^{-2}$ . Wind speeds are on average similar between the two wind phenomena, and thus the substantial difference in heat flux between reverse tip jets and westerlies can be attributed to the associated air temperatures.

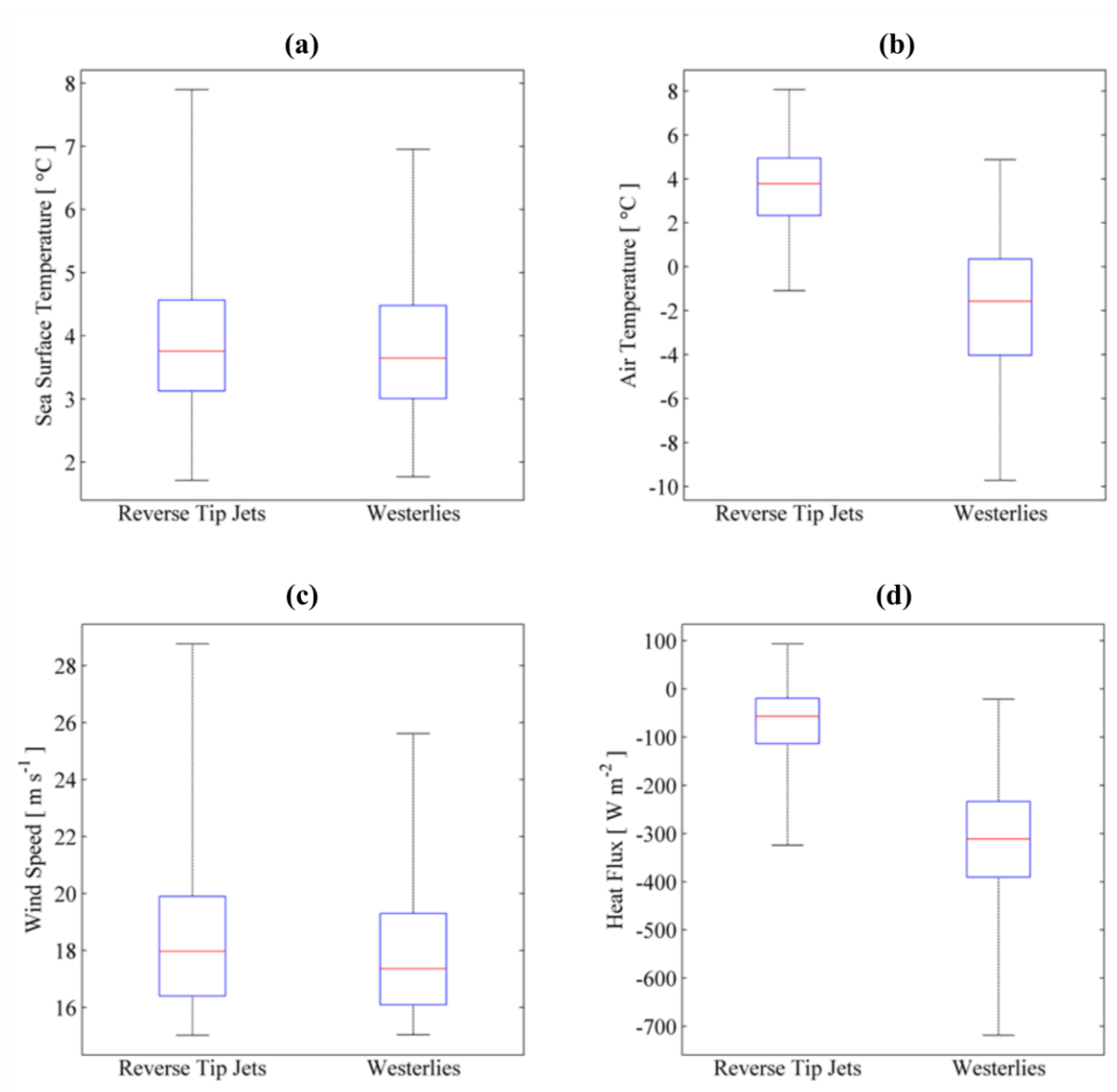


**FIGURE 9:** Boxplots of SST, air-temperature, wind speed, and heat flux for all reverse tip jet and westerly events in winters 2002-2009. The boxplots show the range (upper and lower black lines), median (red line) and the 25<sup>th</sup> and 75<sup>th</sup> percentiles (upper and low bounds of blue box) for: (a) SST (°C), (b) air temperature (°C), (c) wind speed ( $\text{m s}^{-1}$ ), and (d) heat flux ( $\text{W m}^{-2}$ ) for all reverse tip jet and westerlies events from winters (October to April) 2002-2009.



Tables 1 and 2 provide further quantification of the air-sea interaction between reverse tip jets, westerlies and the southeast Labrador Sea for each winter. Composite analysis has enabled the identification of heat fluxes, air temperatures and SST's during both wind phenomena. This allows for the calculation of; total winter duration of reverse tip jets and westerlies, the mean negative heat flux of all reverse tip jet and westerly events within each winter respectively, and the total heat flux contribution by the reverse tip jets and westerlies to the total winter heat flux for each winter. Corresponding with the result in Figure 9, westerlies are the greater contributor to the total wintertime heat flux than reverse tip jets. On average westerlies contribute to 19% of the total winter heat flux in the southeast Labrador Sea, whilst reverse tip jets on average contribute only 2.7%. Quantities provided by composite analysis (Tables 1 and 2) further confirm that air temperature associated with events is the primary factor influencing the considerable difference between mean reverse tip jet heat flux and mean westerly heat flux.

**TABLE 1:** Quantities of reverse tip jet and Labrador Sea air-sea interactions. Values in the right hand columns are winter (October-April) values for the factors stated in the left hand column. Quantities are provided for winters 2002/2003-2008/2009.

<b>Winter (Oct-Apr)</b>	<b>02/03</b>	<b>03/04</b>	<b>04/05</b>	<b>05/06</b>	<b>06/07</b>	<b>07/08</b>	<b>08/09</b>
Total winter reverse tip jet duration (days)	12	16	12	15.5	15	9.5	13
Mean reverse tip jet heat flux ( $W m^{-2}$ )	-55.6	-59.1	-17.2	-42.6	-62.9	-52.2	-12.7
Average wind speed of reverse tip jets ( $m s^{-1}$ )	18.5	18.8	17.8	19.1	18.9	18.0	18.4
Average associated air temperature ( $^{\circ}C$ )	3.6	3.7	3.7	3.6	3.9	3.6	3.6
Average associated sea surface temperature ( $^{\circ}C$ )	4.2	4.6	3.8	3.6	4.4	4.1	3.5
Total winter reverse tip jet heat flux contribution ( $W m^{-2}$ )	-1334.1	-1892.5	-411.8	-1320.3	-1887.4	-992.6	-330.8
Total winter heat flux (all time steps ( $W m^{-2}$ ))	-43649.6	-35871.5	-40320.2	-41335.9	-48180.6	-57615.8	-46374.9
Reverse tip jet % contribution to total heat flux	3.1%	5.3%	1.0%	3.2%	3.9%	1.7%	0.7%

**TABLE 2:** Quantities of westerly and Labrador Sea air-sea interactions. Values in the right hand columns are winter (October-April) values for the factors stated in the left hand column. Quantities are provided for winters 2002/2003–2008/2009.

Winter (Oct-Apr)	02/03	03/04	04/05	05/06	06/07	07/08	08/09
Total winter westerly duration (days)	16.5	14	19	11.5	13	21	18
Mean westerly heat flux ( $\text{W m}^{-2}$ )	-250.0	-220.4	-254.1	-258.4	-241.1	-300.7	-305.8
Average wind speed of reverse tip jets ( $\text{m s}^{-1}$ )	17.9	17.9	18.1	17.8	17.5	18.0	18.0
Average associated air temperature ( $^{\circ}\text{C}$ )	-1.6	-0.9	-1.9	-0.6	-1.8	-2.7	-1.2
Average associated sea surface temperature ( $^{\circ}\text{C}$ )	3.9	4.0	4.0	4.1	3.7	3.5	4.0
Total winter westerly heat flux contribution ( $\text{W m}^{-2}$ )	-8250.8	-6171.0	-9655.4	-5943.5	-6267.5	-12628.0	-11007.5
Total winter heat flux (all time steps ( $\text{W m}^{-2}$ ))	-43649.6	-35871.5	-40320.2	-41335.9	-48180.6	-57615.8	-46374.9
Westerly % contribution to total heat flux	18.9%	17.2%	24.0%	14.4%	13.0%	21.9%	23.7%

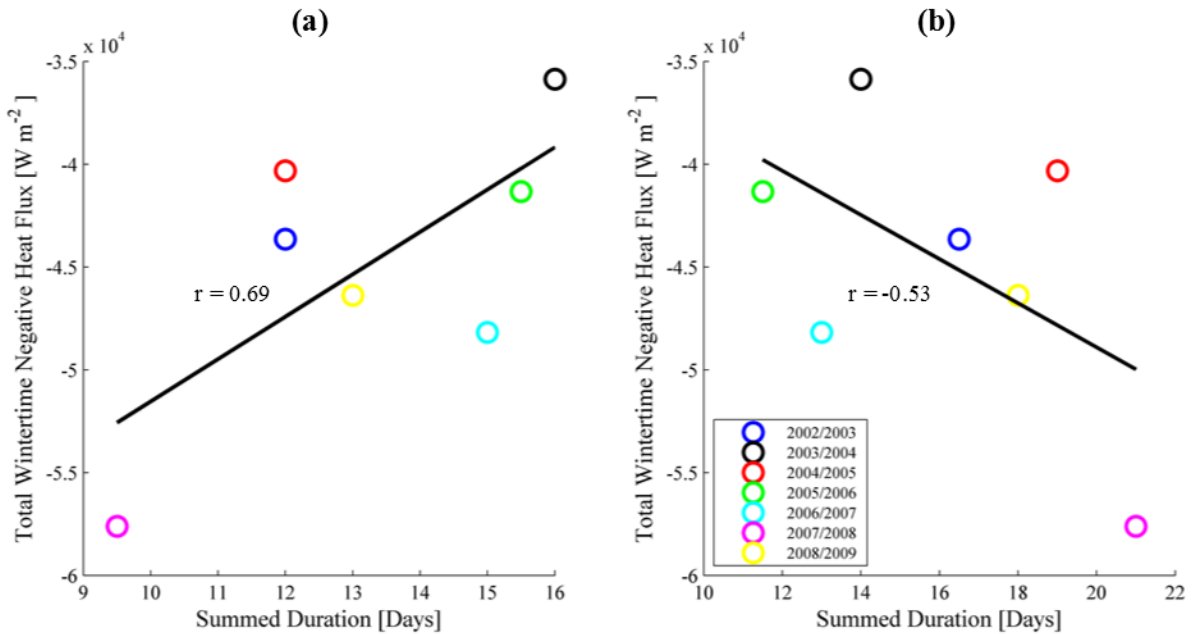


**FIGURE 10:** Scatter plot comparing total winter duration of reverse tip jets (a) and westerlies (b) to the total wintertime negative heat flux from the region of the southeast Labrador Sea for all winters of the study period 2002/2003 to 2008/2009. The total wintertime duration of events is measured by sum of the lengths of all events in each particular winter (units of days).

Statistical analysis of the relationship between the total winter duration of reverse tip jets, westerlies and the total negative heat flux in each winter further highlights the influence these wind events have on winter cooling (Figure 10). The total wintertime duration of events is correlated to total wintertime heat fluxes for reverse tip jets ( $r = 0.69$ ) and westerlies ( $r = -0.53$ ). The results from Table 1 suggests that reverse tip jets have little influence in enhancing negative heat fluxes, as seen by the negligible contribution to the total winter negative heat flux. However, reverse tip jets show a strong positive relationship ( $p = 0.09$ ) suggesting the total wintertime negative heat flux is reduced with increasing reverse tip jet occurrence. Westerlies however, have a negative relationship ( $p = 0.22$ ) indicating that the winter heat loss from the ocean is greater when westerly occurrence is high. Additionally to this, there is considerable variation in the duration of reverse tip jets and westerlies as well as the total heat flux between winters, suggesting the presence of a driving mechanism influencing interannual climate variability.

5.2 INTERANNUAL VARIABILITY

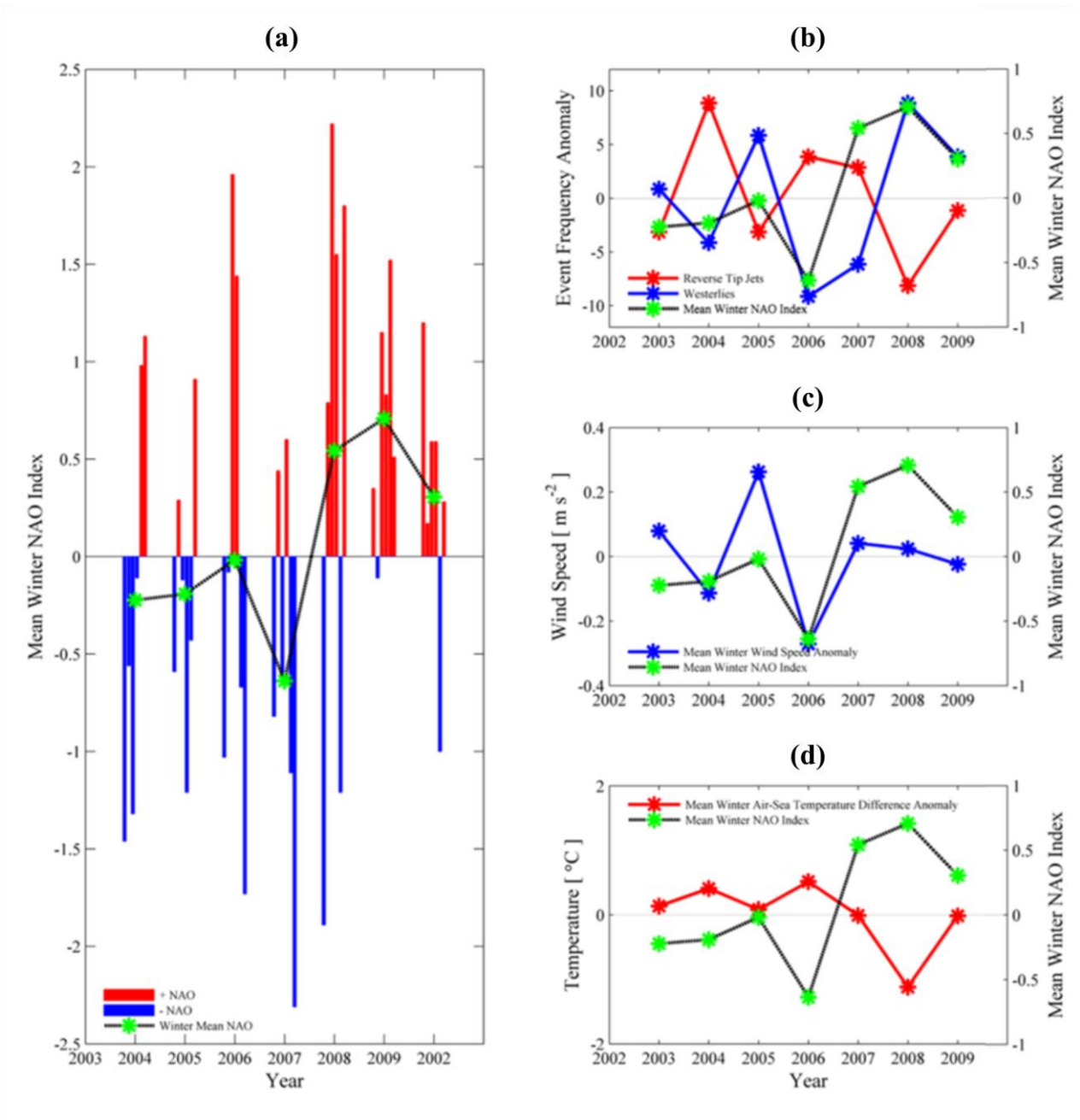


FIGURE 11: Interannual variability of the winter NAO index, reverse tip jet and westerly frequency, mean winter wind speed, and mean winter air-sea temperature difference. For plot a positive NAO (+NAO) is displayed as red and a negative NAO (-NAO) as blue. The value for average winter NAO index is represented by the green stars. Plot b compares the winter average NAO index to the frequency anomaly of reverse tip jets and westerlies. The mean winter wind speed is compared to winter mean NAO in plot c, and the mean winter air-sea temperature difference is compared to winter average NAO in plot d.

The NAO is a dominant pattern of climate variability in the North Atlantic, and therefore is explored to identify its influence on the interannual variability of reverse tip jets, westerlies and the wintertime cooling in the southeast Labrador Sea (Figure 11). The total reverse tip jet heat flux anomaly has a negligible positive correlation to the NAO index (Figure 12 (b),  $r = 0.14$ ,  $p = 0.76$ ), whilst the westerly total heat flux contribution correlates negatively to the NAO (Figure 12(c),  $r = -0.61$ ,  $p = 0.15$ ). Additionally, the total winter heat flux is correlated with the winter NAO index at the 95% level (Figure 12(a),  $r = -0.79$ ) suggesting the NAO is an influence on the general winter climate as well as high speed wind events such as the westerlies. These results determine that +NAO winters coincide with an increased ocean-atmosphere cooling. Winter 2007/2008, a year of strong +NAO index (winter mean = 0.71), experienced the strongest negative heat flux from the southeast Labrador Sea ( $-57615.8 \text{ W m}^{-2}$ ) off all seven winters. Westerlies were also most frequent in this winter (42 events), with the highest contributed heat flux of all seven winters ( $-12628 \text{ W m}^{-2}$ ). However, the heat flux contribution of reverse tip jets has little significance with the NAO (Figure 12(b)). Interestingly, for 2007/2008 reverse tip jets are the least frequent of all seven winters (Figure 11(b)), and the positive correlation between summed duration of reverse tip jets and total winter heat flux (Figure 10(a),  $r = 0.69$ ) suggests that less reverse tip jets coincide with greater negative heat fluxes. This could imply a reduction in reverse tip jet frequency aided the anomalously high negative heat flux, whereby reverse tip jets did not dampen the impact on the ocean-atmosphere heat fluxes.

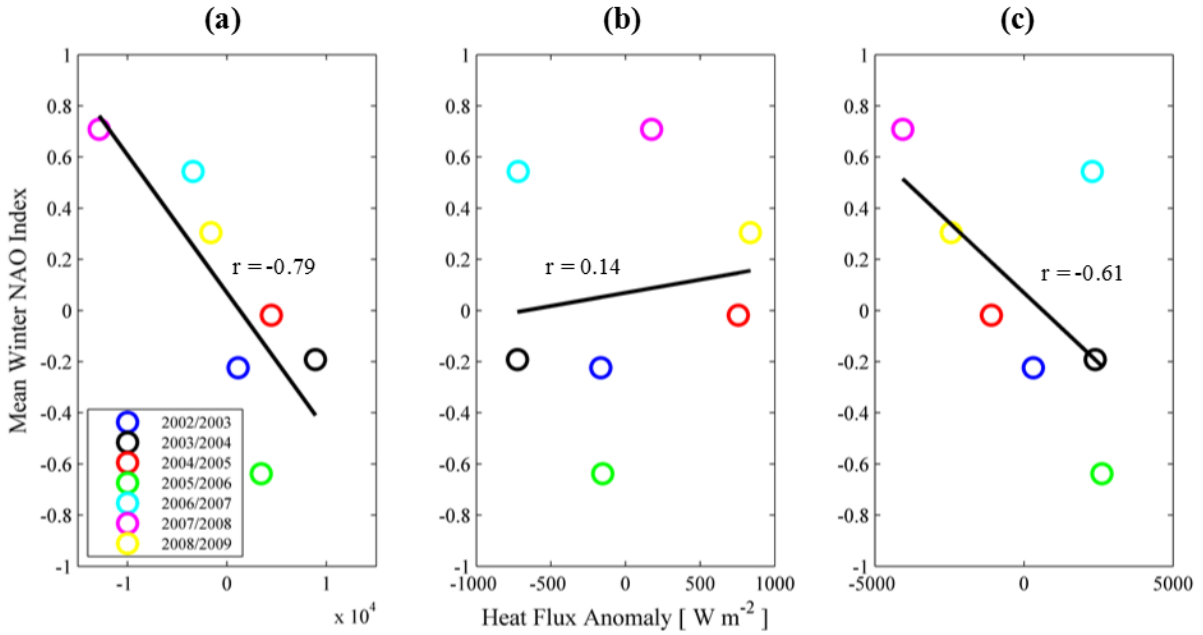


FIGURE 12: Scatter plot comparing winter NAO index with wintertime heat fluxes for winters 2002-2009. Plot a shows the total winter heat flux anomaly ( $W m^{-2}$ ), plot b shows reverse tip jet heat flux contribution anomaly ( $W m^{-2}$ ), and plot c shows westerly heat flux contribution anomaly ( $W m^{-2}$ ). Anomalies are calculated by subtracting the average heat flux of all winters associated with each subplot.

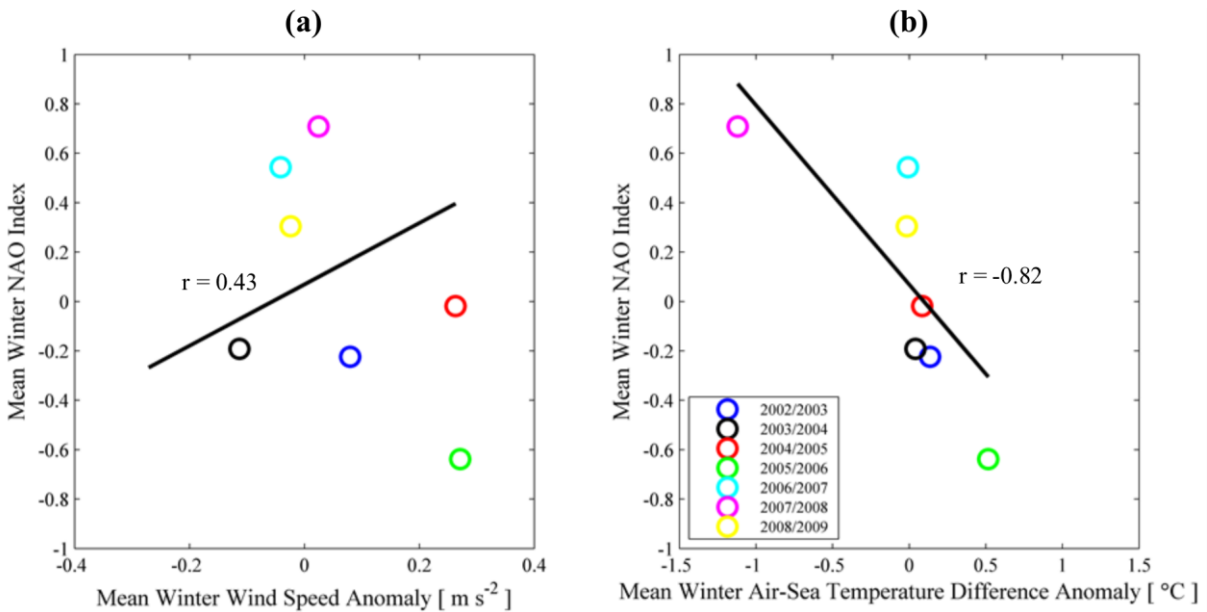


FIGURE 13: Scatter plots comparing mean winter wind speeds and mean air-sea temperature differences with the mean winter NAO index for winter 2002-2009. Plot a shows the mean winter wind speed anomaly ( $m s^{-1}$ ) compared to mean winter NAO index and plot b shows the mean winter air-sea temperature difference anomaly ( $^{\circ}C$ ). Anomalies are calculated by subtracting the average wind speed/temperature difference of all winters associated with each subplot.

Figure 11(c and d) show relationships between the NAO index, mean winter wind speed and mean winter air-sea temperature difference. As the NAO has an opposing impact on the contributed heat fluxes of the reverse tip jets and westerlies, these figures instead examine the NAO's association with general wintertime atmospheric conditions including all weather conditions over the winter period. The NAO has a weak positive relationship with wind speed (Figure 13(a),  $r = 0.43$ ) but a significant negative correlation with the air-sea temperature difference (Figure 13(b),  $r = -0.82$ ). From this we conclude the relatively small percent contributions of reverse tip jets to the total wintertime negative heat flux are due to the origin of these winds. The maritime air from the east is warmer than that from the Canadian continent which feed the westerlies (Figure 9(b)). Westerlies contribute to a greater portion of the total wintertime heat flux, especially in favourable +NAO conditions, but a large portion of the ocean-atmosphere cooling is not accounted for. The weak relationship between wind speed and the winter NAO index implies that the high speed wind events are not the dominant factor in wintertime cooling over the Labrador Sea. Our results instead suggest that the air-sea temperature difference is the driving influence behind strength of ocean-atmosphere heat fluxes. This indicates large scale atmospheric conditions not associated with high speed events are the primary driver of heat loss from the southeast Labrador Sea. However, in favourable climatic conditions such as +NAO, the combination of colder atmospheric temperature and a high frequency of westerlies can drive anomalously strong winter negative heat fluxes from the southeast Labrador Sea, such as that in winter 2007/2008. However, as these relationships are specific to the southeast Labrador Sea, the impact of NAO on the surrounding region needs further analysis.

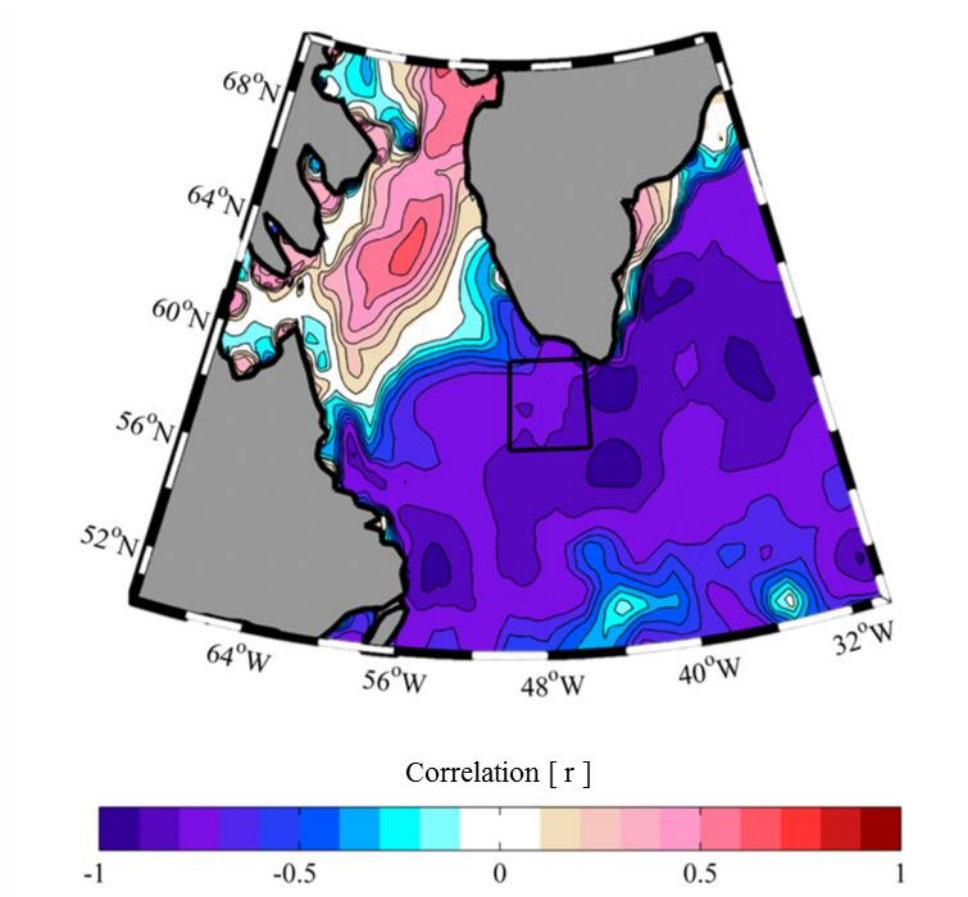


FIGURE 14: Correlation contour plot of winter mean winter NAO index and the total winter heat flux. The mean winter NAO index is compared with the total winter heat flux ( $\text{W m}^{-2}$ ) at every 0.25 degree interval for the winters inclusive of 2002 to 2009 and plotted as correlation value  $r$ . The black box indicated the location of the southeast Labrador Sea.

Spatial pattern of correlation between winter NAO index and total winter negative heat flux show a large band of anticorrelation running zonally south of Greenland (Figure 14). The strongest relationship is found directly south of Cape Farewell. Here the winter heat flux is strongly influenced by the phase of the NAO ( $r = -0.97$ ) with significance at the 95% level, by which a +NAO will enhance ocean-atmosphere heat fluxes. The location of the strong negative relationship is the exact point at which tip jets form, and would suggest that the NAO is influential on tip jet formation whereby more tip jets leads to stronger negative heat fluxes. Winter 2007/2008 highlights this as westerlies were more frequent than in any other year (Table 2), providing for enhanced forward tip jet formation. The +NAO conditions influence cold atmospheric temperatures and thus drive stronger ocean-atmosphere heat fluxes. Another



area of interest is the northwest Labrador Sea, where a reasonably strong positive correlation is shown (maximum  $r = 0.7$ ,  $p = 0.08$ ). This would suggest that a +NAO influences an atmosphere-ocean heat flux, whereby the atmosphere is cooled by the underlying northwest Labrador Sea, a location known to be the site of winter sea ice.

The spatial distributions of mean air-sea temperature difference anomalies associated with reverse tip jet events and westerlies further highlight the fundamental difference between the wind phenomena and their patterns of interannual variability (Figures 15 and 16). Reverse tip jets are generally associated with low air-sea temperature differences, where air temperatures are warmer during reverse tip jet events than the average winter time temperatures. The warm colours present these low air-sea temperature differences (Figure 14). For the majority of winters (Figure 15(a, c-e, g)) reverse tip jets have on average a relatively warm temperature anomaly, meaning air temperatures and SST are similar with minimal deviation. The spatial pattern of warm temperature anomalies extends meridionally into northern Labrador Sea and Baffin Bay, with a larger scale zonal extension into the North Atlantic Ocean. The average air-sea temperature difference anomaly for all reverse tip jets in all winters studied (2002-2009) also shows this pattern (Figure 15(h)). However, for winter 2003/2004 (Figure 15(b)) this spatial pattern is restricted to the Labrador Sea. Winter 2007/2008 is the most anomalous (Figure 15(g)), where a band of  $-2\text{ }^{\circ}\text{C}$  temperature anomaly occurs in the northern Labrador Sea parallel with the coast. This suggests a strong presence of sea ice which is colder than the average air temperatures above. The continental land temperatures throughout the winter period are also anomalously cold compared to other winters, and therefore why we see a large spatial distribution of positive temperature anomalies across the Canadian continent.

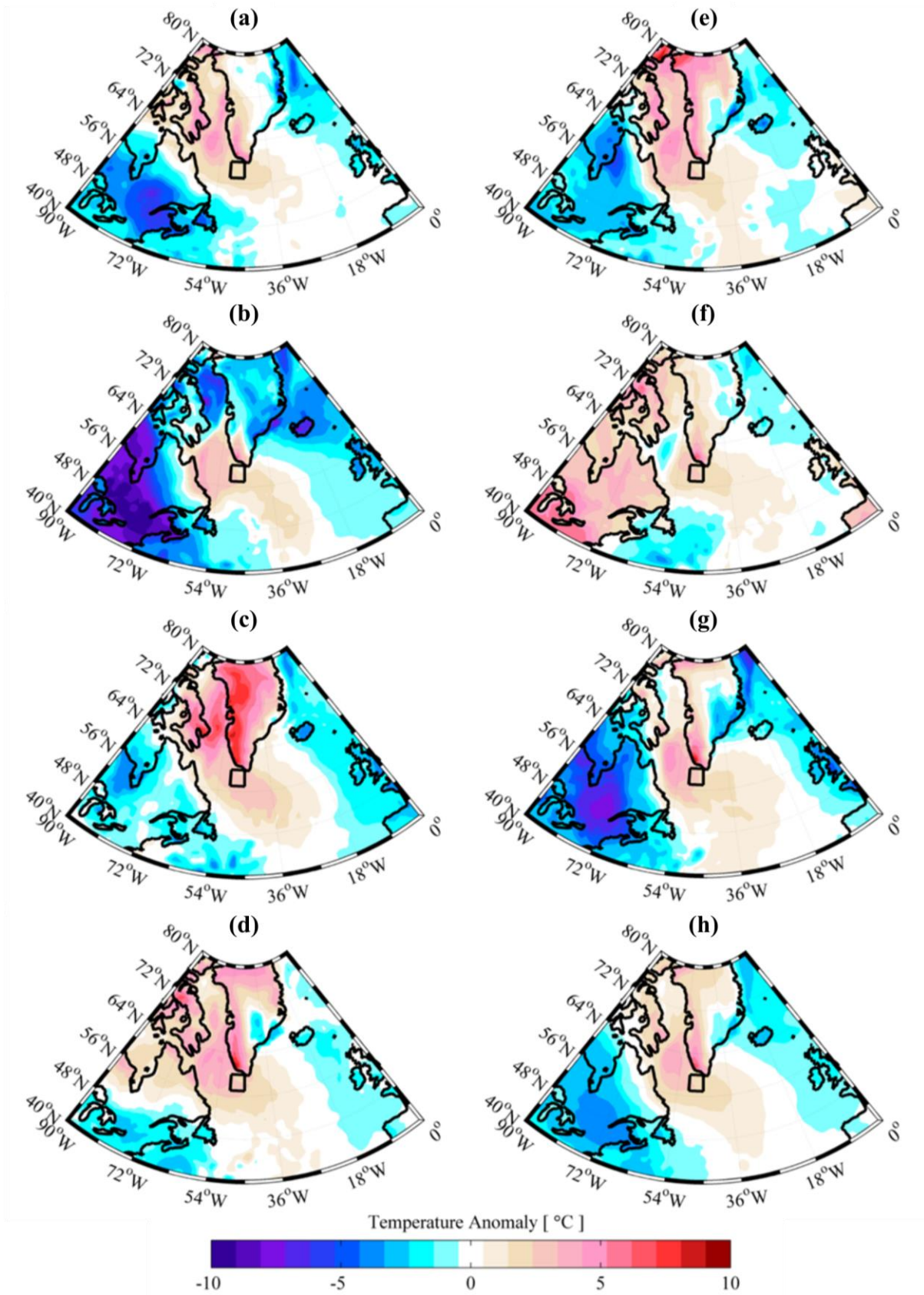


FIGURE 15: Mean air-sea temperature difference anomalies associated with reverse tip jets for winter periods. Plots a-g are Winters 2002/2003-2008/2009, and plot h is an average of all seven winters. Warm colors represent smaller air-sea temperature differences than the mean winter air-sea temperature difference for winters 2002-2009.

On the contrary, the mean westerly air-sea temperature difference anomalies are inverse of those seen for reverse tip jets (Figure 16). Westerly spatial patterns are dominated by cold colours representing a negative temperature anomaly where air temperatures are far cooler than surface temperatures, whilst being generally colder than the average winter time conditions. The spatial pattern of negative temperature anomalies extend from the western continent across the entire Labrador Sea, then further into the North Atlantic Ocean to the east. This pattern is clearly seen in the average anomaly of all westerly events from all winters studied (Figure 16(h)). Winter 2007/2008 shows the longest extension of strong negative temperature anomaly (Figure 15(f)), with a large  $-4\text{ }^{\circ}\text{C}$  air-sea temperature difference extending across the southeast Labrador Sea to a longitude of  $34\text{ }^{\circ}\text{W}$ . The large air-sea temperature difference anomaly of 2007/2008 coincides with strongest total winter heat flux of all winters studied. Fundamentally, the westerlies are sourced from the cold Canadian continent and have greater air-sea temperature differences than average winter conditions. Reverse tip jets originate from warmer maritime waters of the North Atlantic and air-sea temperature differences are smaller than average winter conditions.

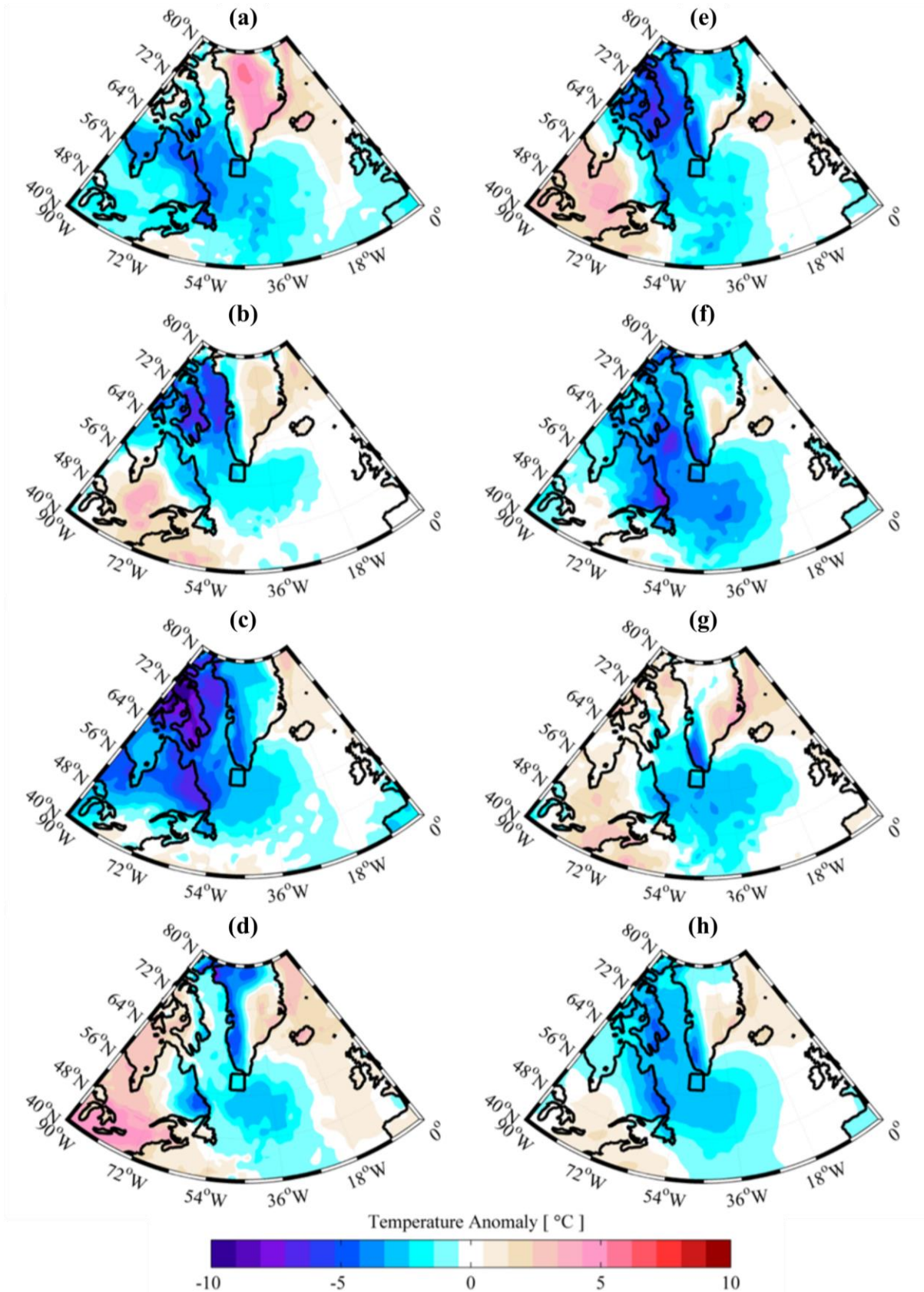


FIGURE 16: Mean air-sea temperature difference anomalies associated with westerlies for winter periods. Plots a-g are Winters 2002/2003-2008/2009, and plot h is an average of all seven winters. Cold colours represent larger air-sea temperature differences than the mean winter air-sea temperature difference for winters 2002-2009.

*Section VI***DISCUSSION****6.1 VALIDATING DATA ACCURACY**

Greenland's tip jets have relatively small spatial scale, and therefore data resolution is a major consideration when creating climatology's of the events. QuikSCAT's 0.25 degree resolution is fine enough to resolve the tip jets for successful identification and analysis, but alternate datasets are also available such as National Centres for Environmental Prediction (NCEP) reanalysis (Moore, 2003) and station observations (Cappelen et al., 2001). The consensus in the scientific community is that QuikSCAT data provides the best estimation of wind speeds compared to alternate satellite and reanalysis datasets. Reanalysis surface wind fields from the NCEP and ECMWF compared to QuikSCAT generally underestimate the intensity of wind speeds (Chelton et al., 2005; Sproson et al., 2010) and thus were a less favourable choice for the analyses of wind speeds made in this study.

The validity of QuikSCAT as the optimum data set for tip jet analysis is also tested through alternate means of measurement such as buoys and aircraft observations. A study by Ebuchi et al. (2002) validated wind vectors from QuikSCAT with data from ocean buoys. The ocean buoy data used were within 30 minutes and 25 km of the equivalent QuikSCAT data, and their results show a good agreement between the buoy and satellite data. RMS differences of  $1.01 \text{ m s}^{-1}$  and  $23^\circ$  were calculated for wind speed and direction respectively. Substantial effort has been made to collect direct measurements of tip jet events through aircraft observations. The Greenland Flow Distortion Experiment (GFDEX) by Renfrew et al. (2008) obtained such observations and prove to be highly comparable to the QuikSCAT data for the tip jet events measured via aircraft observations (Renfrew et al., 2009).

A final methodology to mention that makes comparison to QuikSCAT wind data are model simulations. Martin and Moore (2007) make a simulation of a robust reverse tip jet that

occurred from the 20<sup>th</sup> to the 23<sup>rd</sup> of December 2000 using the Penn State-NCAR Mesoscale Model version 5 with data from the Canadian Meteorological Centre analysis data. This event was one of the strongest found in Moore and Renfrew's (2005) climatology with peak wind speeds of over 40 m s<sup>-1</sup>. However, the model simulation of the event does under predict the wind speeds by up to 10 m s<sup>-1</sup> suggesting issues with model parameterization. In light of this, current efforts are being made to force resolving of tip jets in relatively low resolution (~1 degree) atmospheric reanalyses such as NCEP and ECMWF which are used to force general circulation models (GCM). Notably, Sproson et al. (2010) have been developing a method of 'bogussing' Greenland's tip jets into such surface wind fields, allowing for incorporation of the mesoscale wind events in GCMs with sufficient resolution. Such methodologies will be important for future work analysing role of Greenland's winds in ocean-atmosphere coupling.

## 6.2 COMPLEXITY OF TIP JETS

A major difficulty in making climatology's and analyses of Greenland tip jets is the variation in their meteorological composition. The time series of tip jets made in this study have shown that no two tip jets are of exactly the same spatial extent, orientation or maximum wind speed, a difficulty also found by Sproson et al. (2010). The method of using specific thresholds and criteria in the composite analysis made in this study were chosen purposely, as the key interest for this study is the overall winter impact multiple tip jets and westerlies have on the Labrador Sea. However, other studies have used more intricate methodologies to make finely tuned characterisations of differing tip jet types. Moore (2014) uses the North American Regional Reanalysis (NARR) to generate a higher resolution climatology of the mesoscale jets than compared to older climatology's such as Moore and Renfrew (2005). The use of a diagnostic that classifies the occurrence frequency of high-speed wind events by their direction shows that four different types of tip jet form off Cape Farewell. The four jet types include north-westerly,

south-westerly, north-easterly, and south-easterly, with the south-westerly and north-easterly jets closely resembling the forward tip jets and reverse tip jets described in this study. Moore (2014) states that there are instances where one type of tip jet evolves into another, and thus for the objective of quantifying their associated heat fluxes it is acceptable to characterise bimodally.

The recent findings of Moore (2014) suggest that the tip jets are more complex than originally supposed, which may explain why the relationship between the frequency of reverse tip jets, westerlies and total winter negative heat flux are weaker than expected. The complexity of these tip jets is induced from a large amount of variation in the atmospheric conditions including; pressure gradients, cyclone activity and storm tracks (Våge et al., 2009a; Moore 2003; Bakalian et al., 2007; Moore et al., 2011). Regardless of a tip jets orientation, all events are a result of interaction between the high topography of Greenland and cyclone activity (Moore, 2014). These cyclones travel along the main North Atlantic storm track, which is known to experience variation from influence by atmospheric phenomena such as NAO and the North Atlantic storm track (Rogers et al., 1990; Hameed et al., 1995). This results in differences in the frequency of westerlies and reverse tip jets (Bakalian et al., 2007; Moore et al., 2011). The impact of these variations in storm track is still not fully understood, but it can be speculated that the storm track will dictate the atmospheric conditions that will either be cold, favouring strong ocean-atmosphere heat fluxes, or relatively warm in which the tip jet will not have a cooling effect. The variation of storm tracks over short time periods could explain some of the variability of reverse tip jets and westerlies found in this study. Variability in the westerly and forward tip jet event shown in Figure 5 is suitable to Moore's (2014) multiple tip jet classification. The forward tip jet orientation is seen to quickly evolve and should be considered as a single continuum consisting of both north-westerly and south-westerly jets (Figure 5(a and c respectively)). Moore (2014) also iterates that the position and

orientation of a particular event will determine the impact it has on local climate and air-sea interaction, suggesting that there is no simple linear relationship between the winter frequency of tip jets and total winter negative heat flux to which they contribute.

### 6.3 ASSOCIATED HEAT FLUXES

As previously discussed, Greenland's tip jets are more complex than initially thought. The variations in spatial extent, orientation and maximum wind speed therefore has a consequent impact of the associated air-sea interactions. A key interest in this study is the ocean-atmosphere heat flux associated with the tip jets, particularly how they impact the southeast Labrador Sea. Previous studies have concluded that forward tip jets provide far greater negative heat fluxes over the Irminger Sea than reverse tip jets do over the Labrador Sea (Pickart et al., 2003; Våge et al., 2009b). This is also seen in the results from analysis made in this study (Figures 4 and 5). Interestingly, our results show that forward tip jets not only drive strong heat fluxes over the Irminger Sea, they also drive strong heat fluxes over the southeast Labrador Sea. For all winters, the westerlies that feed the forward tip jets provide larger contribution to the total negative winter heat flux of the southeast Labrador Sea than the reverse tip jets. This raises the question of how important are the strength of the winds? Our results have demonstrated that the combination of strong winds with a large air-sea temperature difference (the air temperature being cooler than SST) provides for strong surface negative heat fluxes. For instance a reverse tip jet that occurred in mid-January of 2003 had maximum wind speeds exceeding  $30 \text{ m s}^{-1}$ , but due to a negligible difference between air and sea temperature the surface heat flux did not exceed  $-100 \text{ W m}^{-2}$ . Alternatively, a forward tip jet that occurred in late January of 2003 had maximum wind speeds of  $20 \text{ m s}^{-1}$ , but associated air temperatures  $9 \text{ }^{\circ}\text{C}$  cooler than the SST lead to a surface heat flux of  $-375 \text{ W m}^{-2}$ , more than double that of the reverse tip jet with faster wind speeds. Other studies suggests that the strong heat fluxes seen



over the southeast Labrador Sea in periods of forward tip jet events is due to large westerly outbreaks of cold air from the coast (Dickson et al., 1996; Renfrew and Moore, 1999; Renfrew et al., 2002). Our results agree with those of Sproson et al. (2008), and are further confirmed by Moore et al. (2014) whom state the large heat fluxes that occur over the eastern Labrador Sea are a result of westerly flow distortion along the southwest coast of Greenland.

Despite the stronger heat fluxes associated with westerlies, there are a few individual cases of reverse tip jets having a cooling influence over the southeast Labrador Sea. Previous studies have investigated these events (Martin and Moore, 2007; Ohigashi and Moore, 2009) and found events with associated heat fluxes of up to  $-150 \text{ W m}^{-2}$ . However, the studies by Martin and Moore (2007) and Ohigashi and Moore (2009) were off singular events and as consequence Sproson et al. (2010) requested that further study needed to be completed for the reverse tip jets and their potential enhancement of heat fluxes to the west of Cape Farewell. The analysis in this study finds only a few reverse tip jet events that drive heat fluxes of up to  $-150 \text{ W m}^{-2}$ , and over entire winters average event heat fluxes are no greater than  $-65 \text{ W m}^{-2}$ . The key to understanding why reverse tip jets have relatively weak associated ocean surface heat fluxes compared to westerlies is due to the origin of the winds. Våge et al. (2009a) used a 3-dimensional Lagrangian trajectory model (Wernli and Davies, 1997) to compute 2-day backward air parcel trajectories terminating to the east of Cape Farewell. The trajectories were selected objectively as those which were the source of a forward tip jet of wind speeds greater than  $20 \text{ m s}^{-1}$ . With nearly 3000 trajectories from 101 forward tip jets from 1994 to 2002, the origin air parcels of these events was over the cold Canadian continent. Cold and dry continental air will extract more heat from the ocean compared to relatively warm and moist maritime area. Analysis by Våge et al. (2009a) clearly shows the trajectories passing over the very cold winter time northern Canadian continent, then passing the western Labrador Sea which at this time of year is covered in sea ice. With trajectories such as these, the westerlies

that feed forward tip jets are very effective at extracting heat from the Labrador and Irminger seas. Comparatively, the warm and moist maritime origins of reverse tip jets are why ocean-atmosphere heat fluxes are far smaller over the Labrador Sea.

#### 6.4 TIP JETS AND THE NAO

Results from this study and others (Moore, 2014; Sproson et al., 2008; Våge et al., 2009a) have found that tip jets are highly variable on an event to event basis. It is also shown that the frequency of events in a winter period is variable from one winter to another. This has important climatic impacts as tip jets are suggested to enhance winter ocean-atmosphere heat fluxes and contribute to the preconditioning of surface waters in the Labrador and Irminger seas for deep convection to occur (Våge et al., 2009b; Pickart et al., 2003). The results from this study have shown that in some years reverse tip jets and westerlies are far more infrequent than in others. For example the total winter duration of reverse tip jets in winter 2002/2003 was 12 days, whilst in winter 2007/2008 it was 9.5 days. The same is true for westerlies with winter 2007/2008 having a winter duration of 21 days but in winter 2006/2007 only 13 days. The link between this variability and NAO has previously been explored (Sproson et al., 2008; Våge et al., 2009b; Pickart et al., 2003) whereby strong correlations were found between the strength of the NAO phase and the frequency of westerlies that occurred. Våge et al. (2009a) determined a correlation of 0.71. Similar analysis of this relationship has been made in this study and found that for the region of southeast Labrador Sea correlation between winter mean NAO and reverse tip jet frequency had a negative relationship ( $r = -0.52$ ,  $p = 0.23$ ), and positive relationship to westerly frequency ( $r = 0.55$ ,  $p = 0.2$ ). These relationships are not significant to the 95% level. This suggests the pathways of the wind events are more variable over the southeast Labrador Sea compared to the east of Cape Farewell at the location of forward tip jet occurrence where Våge et al. (2009a) made their analysis. However, the findings of Våge et al.

(2009a) compare well to other results of this study (Figure 14). The region directly south of Cape Farewell shows a strong negative relationship significant at the 95% level between winter mean NAO and winter total negative ocean surface heat flux ( $r = -0.97$ ). The location of this significant positive correlation suggests that a +NAO coincides with strong ocean-atmosphere heat fluxes, which in turn can be related to a greater frequency of tip jets forming at this location. This relationship is also apparent for the southeast Labrador Sea, where a +NAO is also significantly correlated with larger negative heat fluxes ( $r = -0.79$ ). However, in the northwest margin of the Labrador Sea there is a reasonably significant positive correlation ( $r = 0.7$ ,  $p = 0.08$ ) implying a strong +NAO is associated with atmosphere-ocean heat flux. This can be explained by the presence of sea ice in the winter period. The waters in the vicinity of sea ice will be colder than those in the southeast Labrador Sea and therefore the sea ice cools the air mass above. Our results suggest favourable +NAO conditions will enhance ocean-atmosphere heat fluxes (up to  $-800 \text{ W m}^{-2}$ ) when westerlies pass over the southeast Labrador Sea. Heat fluxes of such magnitude have potential to trigger deep convection.

## 6.5 INFLUENCING DEEP CONVECTION

The onset of deep convection is thought to follow suitable preconditioning of the water column (Våge et al., 2009a). Taking the example of winter 2007/2008, Våge et al. (2009a) found that air-sea heat fluxes in the Labrador and Irminger seas were comparatively weak in the previous winter. Our results also imply this where the total negative winter heat flux from southeast Labrador Sea was 16.4% lower in winter 2006/2007 compared to 2007/2008 (Table 2). This suggests that there was relatively little remnant convected water from previous winters, and the deep convection that occurred in winter 2007/2008 is a product of vigorous storm activity. The results from this study agree with Yashayaev and Loder (2009) who have shown that winter 2007/2008 had the largest cumulative heat loss from the Labrador Sea to the atmosphere from

2000-2008. They continue to suggest the high level of atmospheric cooling is the cause of enhanced LSW production in that particular winter. It would seem a combination of +NAO with cold associated atmospheric temperatures and a higher frequency of westerlies than in the previous 5 winters enhanced the ocean-atmosphere heat flux, influencing the surprising return of deep convection in 2007/2008 (Våge et al., 2009b). Our results also suggest reverse tip jets are incapable driving deep convection. Sproson et al., (2008) also found that reverse tip jets have relatively low negative heat fluxes and in some cases for the winter 1996/1997 the air temperatures associated with the jets were warm enough to induce a positive heat flux from atmosphere to ocean. They continue to compare NAO with heat fluxes associated with reverse tip jets from strong +NAO winter 1994/1995 and a strong -NAO winter 1995/1996, and in both cases the heat fluxes were below the wintertime average, regardless of NAO phase.

Analysis by Våge et al. (2009b) highlights that storm tracks are a key feature in the provision of the strong cooling in winter 2007/2008. The storm track was more favourable for westerlies, whereby the cyclones followed a well-defined track from the Canadian continent towards the Irminger Sea. With such a track, the topography of Greenland distorts the synoptic scale flow of the cyclones to force forward tip jet formation. Våge et al. (2009b) also suggests that shifts in the storm track can have reducing consequences for tip jet formation regardless of the NAOs phase. A more south-westerly track will cause cyclones to bypass the west coast of Greenland consequently reducing the level of distortion and tip jet formation. This study demonstrates that the comparatively warm reverse tip jets cannot provide the necessary cooling for deep convection in the region of the southeast Labrador Sea. However, cold westerlies in combination with high frequency of occurrence and optimum climatic conditions (favourable NAO and storm track) have the potential to enhance LSW formation over the central and southeast Labrador Sea. Interestingly, the westerly events are also the parent weather system for forward tip jet formation. The most robust forward tip jets are shown to have strong enough

winds for turbulent mixing, and cold associated air temperatures that drive cooling and deep convection in the Irminger Sea without preconditioning (Pickart et al., 2003; Våge et al., 2009b).

*Section VII***CONCLUSIONS**

QuikSCAT surface wind data has been used for the successful objective identification of reverse tip jet and westerly events over seven winter periods (October-April) from 2002-2009. Results show reoccurrence of reverse tip jets forming over the southeast Labrador Sea. Synoptic scale westerlies from the Canadian continent also occur at this location before forming forward tip jets over the Irminger Sea. ERA-I heat flux fields, air temperature and SST have also been used in composite analysis to identify the associated air-sea interactions between reverse tip jets, westerlies and the southeast Labrador Sea. For the purpose of identifying associated air-sea interactions this method is successful. However, the tip jets are shown to be meteorologically more complex than a bimodal phenomenon. Both reverse tip jets and westerlies vary directionally over a singular event suggesting future climatology's should classify tip jets into 4 categories (Moore, 2014).

Reverse tip jets and westerlies have considerably different associated heat fluxes. Reverse tip jets have relatively weak associated ocean-atmosphere heat fluxes, with robust events driving negative heat fluxes of up to no greater than  $-150 \text{ W m}^{-2}$  over the southeast Labrador Sea. The westerly events drive the strongest heat fluxes over the southeast Labrador Sea of up to  $-720 \text{ W m}^{-2}$ , which can additionally form into forward tip jets that drive equally strong ocean-atmosphere heat fluxes over the Irminger Sea. Air-sea temperature differences are determined as the primary of driver ocean-atmosphere heat fluxes in tip jet and westerly events. The source region of atmospheric masses that feed reverse tip jets and westerlies are found to be the key factor in determining associated air temperature and the strength of heat flux over the southeast Labrador Sea. The outbreaks of air from the Canadian continent are significantly colder than the surface waters of the southeast Labrador Sea, whilst the warm maritime air from the east that feeds the reverse tip jets are rarely cooler than the surface waters.

Variability of reverse tip jets, westerlies and their associated air-sea interactions are also shown over interannual time scales. Our results show that the NAO has a negative relationship ( $r = -0.61$ ) with westerly contribution to total negative wintertime heat flux over the southeast Labrador Sea. This indicates an increase in frequency of westerlies drives greater cooling in favourable +NAO conditions. Heat flux contribution by reverse tip jets has no significant relationship with the NAO, but reverse tip jet frequency has a positive relationship with the total winter time heating ( $r = 0.69$ ) suggesting these wind events have a dampening impact on wintertime cooling. For winter 2007/2008 a combination of cold +NAO atmospheric conditions and a high frequency of westerly occurrences coincided with the surprising return of deep convection, highlighting westerlies an important contributor to wintertime cooling in the Labrador Sea.

Due to the relatively warm air temperatures associated with reverse tip jets it is confirmed they are not capable of driving deep convection in the southeast Labrador Sea. However, it must be noted reverse tip jets are strong and complex wind phenomena with a primary influence on local ocean circulation, which is still little understood. The potential for the changing climate to be accompanied by a poleward shift of the North Atlantic storm track will have important consequences on the frequency of extreme wind phenomena in the vicinity of Cape Farewell. This further highlights the necessity to better understand the role of westerlies as a contributor to deep convection. It is recommended that future studies investigate the extent to which variations in the North Atlantic storm track influence the frequency, formation and associated air-sea interactions of westerlies over locations sensitive to global climate such as the Labrador and Irminger seas.

## REFERENCES

- Bakalian, F., Hameed, S., and Pickart, R. (2007). Influence of the Icelandic Low latitude on the frequency of Greenland tip jet events: Implication for Irminger Sea convection. *Journal of Geophysical Research*. 112, 1-6.
- Berrisford, P., Dee, D., Poli, P., Brugge, R., Fielding, K., Fuentes, M., Kållberg, K., Kobayashi, S., Uppala, S and Simmons, A. (2011). The ERA-Interim archive: Version 2.0. *European Centre for Medium Range Weather Forecasts*: Reading, United Kingdom. 1-23.
- Cappelen, J., Jorgensen, B.V., Laurensen, E.V., Stannius, L.S., and Thomsen, R.S. (2001). The observed climate of Greenland, 1958-1999, with climatological standard normal. 1961-1999. *Danish Meteorological Institute Tech. Rep.* 00-18, 149.
- Chelton, D.B., Freilich, M.H., Sienkiewicz, J.C., and Von Ahn, J.M. (2006). On the Use of QuikSCAT Scatterometer Measurements of Surface Winds for Marine Weather Prediction. *Monthly Weather Review*. 134, 2055-2071.
- Clark, R.A., and Gascard, J.C. (1983). The formation of Labrador Sea water. Part I: Large-scale processes. *Journal of Physical Oceanography*. 13(10), 1764-1778.
- Dee, D.P., Uppala, S.M., Simmons, A.J., Berrisford, P., Poli, P., Kobayashi, S., Andrea, U., Balmaseda, M.A., Balsamo, G., Bauer, P., Bechtold, P., Beiljaars, A.C.M., van de Berg, L., Bidlot, J., Bormann, N., Delsol, C., Dragani, R., Fuentes, M., Geer, A.J., Haimberger, L., Healy, S.B., Hersbach, H., Hólm, E.V., Isaksen, I., Kållberg, P., Köhler, M., Matricardi, M., McNally, A.P., Mogné-Sanz, B.M., Morcrette, J.J., Park, B.K, Peubey, C., de Rosney, P., Tavolato, C., Thépaut, J.N., and Vitart, F. The ERA-Interim reanalysis: configuration and performance of the data assimilation system. *Quarterly Journal of the Royal Meteorological Society*. 137, 553-597.
- Dickson, B., Yashayaev, I., Meincke, J., Turrell, B., Dye, S., and Holfort, J. (2002). Rapid freshening of the deep North Atlantic Ocean over the past four decades. *Nature*. 416(6883), 832-837.
- Dickson, R., Lazier, J., Meincke, J., Rhines, P., and Swift, J. (1996). Long-term coordinated changes in the convective activity of the North Atlantic. *Progress in Oceanography*. 38. 241-295.
- Doyle, J.D., and Shapiro, M.A. (1999). Flow response to a large scale topography: The Greenland tip jet. *Tellus Series*. 51, 728-748.
- DuVivier, A.K., and Cassano, J.J. (2015). Exploration of turbulent heat fluxes and wind stress curl in WRF and ERA-Interim during wintertime mesoscale wind events around southeastern Greenland. *Journal of Geophysical Research*. In Press, 1-46.
- Ebuchi, N., Graber, H.C., and Caruso, M.J. (2002). Evaluation of Wind Vectors by QuikSCAT/SeaWinds Using Ocean Buoy Data. *Journal of Atmospheric and Oceanic Technology*. 19, 2049-2062.
- Hameed, S., Shi, W., Boyle, J., and Santer, B. (1995). Investigation of the centers of action in the North Atlantic and North Pacific in the ECHAM AMIP simulation. In: *Proceedings of the First International AMIP Scientific Conference, Monterey, California WCRP-92, WMP/TD-732*. World Climate Research Programme, Geneva. 221-226.
- Harden, B.E., Renfrew, I.A., and Petersen, G.N. (2011). A Climatology of Wintertime Barrier Winds off Southeast Greenland. *Journal of Climate*. 24, 4701-4717.
- Hartmann, D.L. (1994). Surface Energy Flux Components over the Oceans. *Global Physical Climatology*. Academic Press: San Diego, California. 4.10, 111-114.
- Hurrell, J.W., Kushnir, Y., Ottensen, G., and Visbeck, M. (2003). The North Atlantic Oscillation: climatic significance and environmental impact. *American Geophysical Union*. 134, 1-179.



- Jahn, A., and Holland, M. M. (2013). Implications of Arctic sea ice changes for North Atlantic deep convection and the meridional overturning circulation in CCSM4-CMIP5 simulations. *Geophysical Research Letters*. 40(6), 12061211.
- Kristjánsson, J.E., and McInnes, H. (1999). The impact of Greenland on cyclone evolution in the North Atlantic. *Quarterly Journal of the Royal Meteorological Society*. 125, 2819-2834.
- Kuhlbrodt, T., Griesel, A., Montoya, M., Levermann, A., Hofmann, M., and Rahmstorf, S. (2007). On the driving process of the Atlantic meridional overturning circulation. *Reviews of Geophysics*. 45, 1-32.
- Lavender, K.L., Davis, R.E., and Owens, W.B. (2002). Observations of Open-Ocean Deep Convection in the Labrador Sea from Subsurface Floats. *Journal of Physical Oceanography*. 32(2), 511-526.
- Lazier, J.R.N., Hendry, R.M., Clarke, R.A., Yashayaev, I, and Rhines, P. (2002). Convection and restratification in the Labrador Sea, 1990-200. *Deep Sea Research*. Part A, 49, 1819-1835.
- Lozier, M.S. (2012). Overturning in the North Atlantic. *Annual Review of Marine Science*. 4, 291-315.
- Marshall, J., and Schott, F. (1999). Open-ocean convection: observations, theory, and models. *Review of Geophysics*. 37, 1-64.
- Martin, R., and Moore, G.W.K. (2007). Air-sea interaction associated with Greenland reverse tip jets. *Geophysical Research Letters*. 35, 1-5.
- Mernild, S. H., and Liston, G. E. (2012). Greenland Freshwater Runoff. Part II: Distribution and Trends. *Journal of Climate*. 25(17), 6015-6035.
- Moore, G.W.K. (2014). Mesoscale Structure of Cape Farewell Tip Jets. *Journal of Climate*. 27, 8956-8965.
- Moore, G.W.K., Pickart, R.S., Renfrew, I.A., and Våge, K. (2014). What causes the location of the air-sea turbulent heat flux maximum over the Labrador Sea? *Geophysical Research Letters*. 41, 3628-3635.
- Moore, G.W.K., and Renfrew, I.A. (2014). A new look at southeast Greenland barrier winds and katabatic flow. *US Climate Variability and Predictability Program Variations*. 12. 1 -19.
- Moore, G.W.K., Pickart, R.S. and Renfrew, I.A. (2011). Complexities in the climate of the subpolar North Atlantic: a case study from the winter of 2007. *Quarterly Journal of the Royal Meteorological Society*. 137, 757-767.
- Moore, G.W.K., Pickart, R.S., and Renfrew, I.A. (2008). Buoy observations from the windiest location in the world ocean, Cape Farewell, Greenland. *Geophysical Research Letters*. 35, 1-5.
- Moore, G.W.K., and Renfrew, I.A. (2005). Tip jets and barrier winds: A QuikSCAT climatology of high-speed events around Greenland. *Journal of Climate*. 18, 3713-3725
- Moore, G.W.K. (2003). Gale force winds over the Irminger Sea to the East of Cape Farewell, Greenland. *Geophysical Research Letter*. 30, 1894.
- Ohigashi, T., and Moore, G.W.K. (2009). Fine structure of a Greenland reverse tip jet: A numerical simulation. *Tellus*. 61A, 512-516.
- Oltmanns, M., Staneo, F., Moore, G.W.K., and Mernild, S.H. (2014). Strong Downslope Wind Events in Ammassalik, Southeast Greenland. *Journal of Climate*. 27(3), 977-993.
- Outten, S.D., Renfrew, I.A., and Petersen, G.N. (2009). An easterly tip jet off Cape Farewell, Greenland. II: Simulations and dynamics. *Quarterly Journal of the Royal Meteorological Society*. 135, 1934-1949.
- Petersen, G.N., Renfrew, I.A., and Moore, G.W.K. (2009). An overview of barrier winds off southeastern Greenland during Greenland Flow Distortion Experiment. *Quarterly Journal of the Royal Meteorological Society*. 135, 1950-1967.

- Petersen, G.N., Ólafsson H, and Kristjánsson, J.E. (2003). Flow in the lee of idealized mountains and Greenland. *Journal of the Atmospheric Sciences*. 60, 2183-2195.
- Pickart, R.S., Våge, K., Moore, G.W.K., Renfrew, I.A., Ribergaard, M.H., and Davies, H.C. (2008). Convection in the western North Atlantic subpolar gyre: Do small-scale wind events matter, in *Arctic-subarctic ocean fluxes: defining the role of the northern seas in climate*, edited by R.R. Dickson, J. Meincke, and P.B. Rhines, pp. 629-652, Springer: Dordrecht, the Netherlands.
- Pickart, R., Spall, M., Ribergaard, M., Moore, G., and Milliff, R. (2003). Deep convection in the Irminger Sea forced by the Greenland tip jet. *Nature*. 424, 152-156.
- Pickart, R.S., Torres, D.J., and Allyn Clarke, R. (2002). Hydrography of the Labrador Sea during active convection. *Journal of Physical Oceanography*. 32, 428-457.
- Renfrew, I.A., Petersen, G.N., Sproson, D.A.J., Moore, G.W.K., Adiwidjaja, H., Zhang, S., and North, R. (2009). A comparison of aircraft-based surface-layer observations over Denmark Strait and the Irminger Sea with meteorological analysis and QuikSCAT winds. *Quarterly Journal of the Royal Meteorological Society*. 135, 2046-2066.
- Renfrew, I.A., Moore, G.W.K., Kristjánsson, Ólafsson, H., Gray, S.L., Petersen, G.N., Bovis, K. Brown, P.R.A., Føre, I., Haine, T., Haine, T., Irvine, E.A., Lawrence, A., Ohigashi, T., Outten, S., Pickart, R.S., Shapiro, M., Sproson, D., Swinbank, R., Woolley, A., and Zhang, S. (2008). The Greenland Flow Distortion Experiment. *American Meteorological Society*. 1308-1324.
- Renfrew, I.A., Moore, G.W.K., Guest, P.S and Bumke, K.A. (2002). Comparison of surface layer and surface turbulent flux observations over the Labrador Sea with ECMWF analyses and NCEP reanalyses. *Journal of Physical Oceanography*. 32, 383-400.
- Renfrew, I.A., and Moore, G.W.K. (1999). An extreme cold air outbreak over the Labrador Sea: Roll vortices and air-sea interaction. *Monthly Weather Review*. 127, 2379-2394.
- Rhein, M., Kieke, D., Hüttl-Kabus, S., Roessler, A., Mertens, C., Meissner, R., Klein, B., Böning, C and Yashayaev, I. (2011). Deep water formation, the subpolar gyre, and the meridional overturning circulation in the subpolar North Atlantic. *Deep Sea Research Part II: Topical Studies in Oceanography*. 58(17), 1819-1832.
- Rogers, J.C. (1990). Patterns of low-frequency monthly sea level pressure variability (1899-1986) and associated wave cyclone frequencies. *Journal of Climate*. 3, 1364-1379.
- Sampe, T., and Xie, S.P. (2007). Mapping high sea winds from space: A global climatology. *Bulletin of the American Meteorological Society*. 88, 1965-1978.
- Sproson, D.A.J, Renfrew, I.A. and Heywood, K.J. (2010). A parameterization of Greenland's tip jets suitable for ocean or coupled climate models. *Journal of Geophysical Research*. 115, 1-16.
- Sproson, D.A.J, Renfrew, I.A., and Heywood, K.J. (2008). Atmospheric conditions associated with oceanic convection in the south-east Labrador Sea. *Geophysical Research Letters*. 35, 16.
- Stouffer, R.J, Yin, J., Gregory, J.M., Dixon, K.W., Spelman, M.J., Hurlin, W., Weaver, A.J., Eby, M., Flato, G.M., Hasumi, H., Hu, A., Jungclaus, J.H., Kamenkovich, I.V., Levermann, A., Montoya, M., Murkami, S., Nawrath, A., Oka, A., Peltier, W.R., Robitaille, D.Y., Sokolov, A., Vettoretti, G., and Weber, S.L. (2006). Investigating the causes of the response of the thermohaline circulation to past and future climate changes. *Journal of Climate*. 19, 1365-1387.
- Stroeve, J. C., Serreze, M. C., Holland, M. M., Kay, J. E., Malanik, J., and Barrett, A. P. (2012). The Arctic's rapidly shrinking sea ice cover: a research synthesis. *Climatic Change*. 110(3-4), 1005-1027.
- Talandier, C., Deshayes, J., Treguier, A. M., Capet, X., Benschila, R., Debreu, L., Dussin, R., Molines, J., and Madec, G. (2014). Improvements of simulated Western North Atlantic current system and impacts on the AMOC. *Ocean Modelling*.

- Våge, K., Spengler, T., Davies, H.C., and Pickart, R.S. (2009a). Multi-event analysis of the westerly Greenland tip jet based upon 45 winters in ERA-40. *Quarterly Journal of the Royal Meteorological Society*. 1-19.
- Våge, K., Pickart, R., Thierry V., Reverdin D., Lee. C., Petrie, B., Angnew, T., Wong, A., and Ribergaard M. (2009b). Surprising return of deep convection to the subpolar North Atlantic Ocean in winter 2007-2008. *Nature Geoscience*. 2, 67-72.
- Våge, K., Pickart, R.S., Thierry, V., Reverdin, G., Lee, C.M., Petrie, B., Agnew, T.A., Wong, A., and Ribergaard, M.H. (2008). Surprising return of deep convection to the subpolar North Atlantic Ocean in winter 2007-2008. *Nature Geoscience*. 2, 67-72.
- Wentz, F., Smith, D.K., Mears C.A., and Gentemann C.L. (2001). Advanced algorithms for QuikScat and SeaWinds/AMSR. *Proceedings of IGARSS*. Sydney, Australia, IEEE, 1079-1081.
- Wernli, H., and Davies H. (1997). A Lagrangian-based analysis of extratropical cyclones. I: The methods and some application. *Quarterly Journal of the Royal Meteorological Society*. 123: 467-489.
- Yashayaev, I., and Loder, J.W. (2009). Enhanced production of Labrador Sea Water in 2008. *Geophysical Research Letters*. 36, 1-7.
- Yashayaev, I., van Aken, H.M., Holliday, N.P, and Bersch, M. (2007a). Transformation of Labrador Sea Water in the subpolar North Atlantic. *Geophysical Research Letters*. 34, 1-8.
- Yashayaev, I., Bersch, M., and van Aken, H.M. (2007b). Spreading of the Labrador Sea Water to the Irminger and Iceland Basins. *Geophysical Research Letters*. 34, 1-8.